Tomography

Marco Marcon

Outline

- 2D Fourier Transform
- 2D Discrete Fourier Transform
- Hough Transform
- From Hough to Radon transform
- Lambert-Beer principle
- Computed Tomography
- Filtered Back Projection
- ART and SART methods
- Multispectral acquisitions
- Phase-contrast Tomography

Fourier series reminder

Example

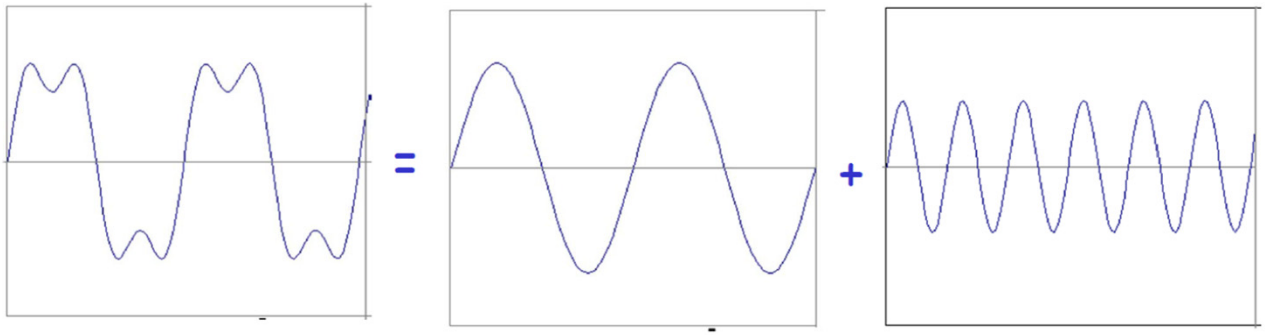

$$f(x) = \sin x + \frac{1}{3}\sin 3x + \ldots$$

Fourier series: just a change of basis

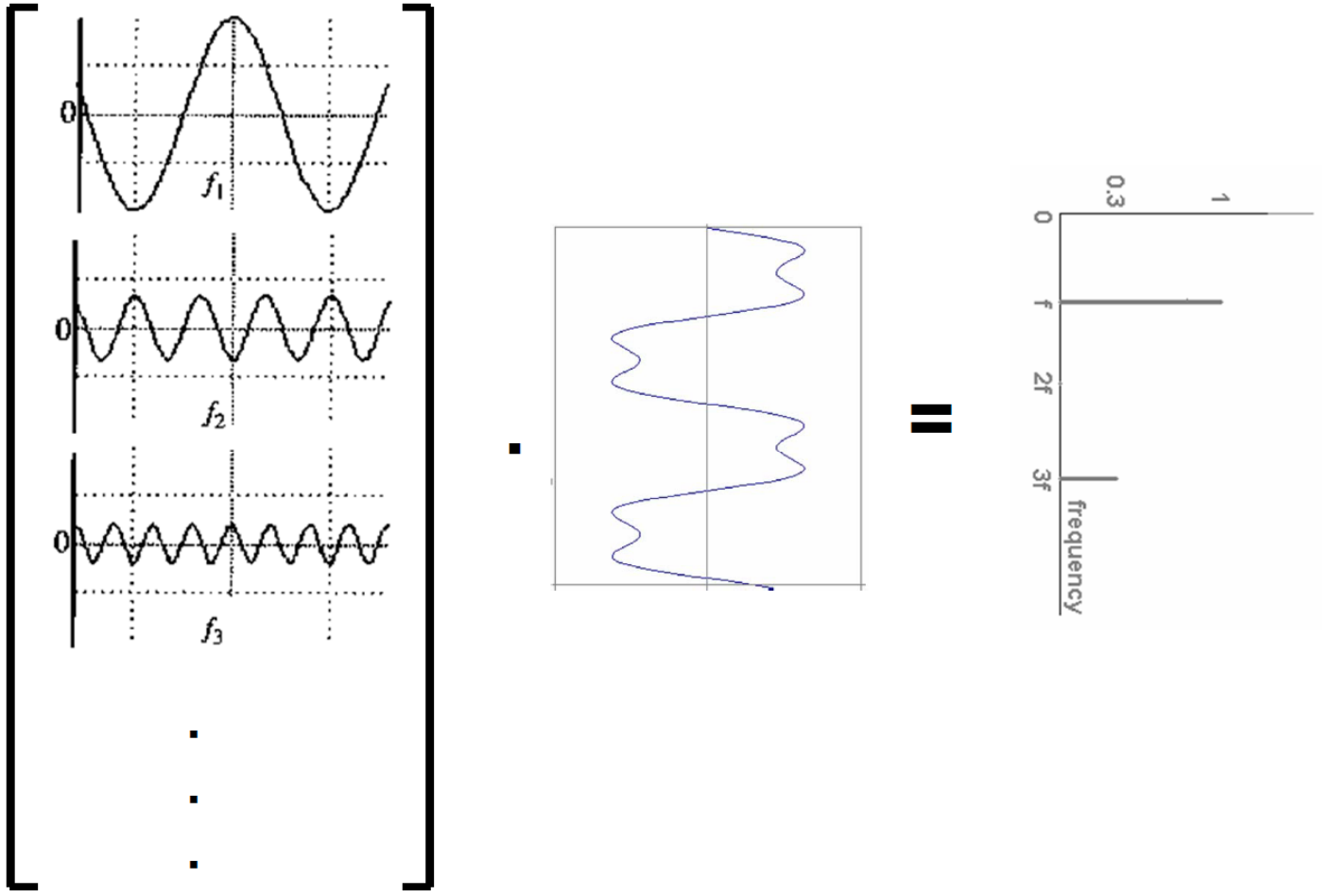

Inverse FT: Just a change of basis

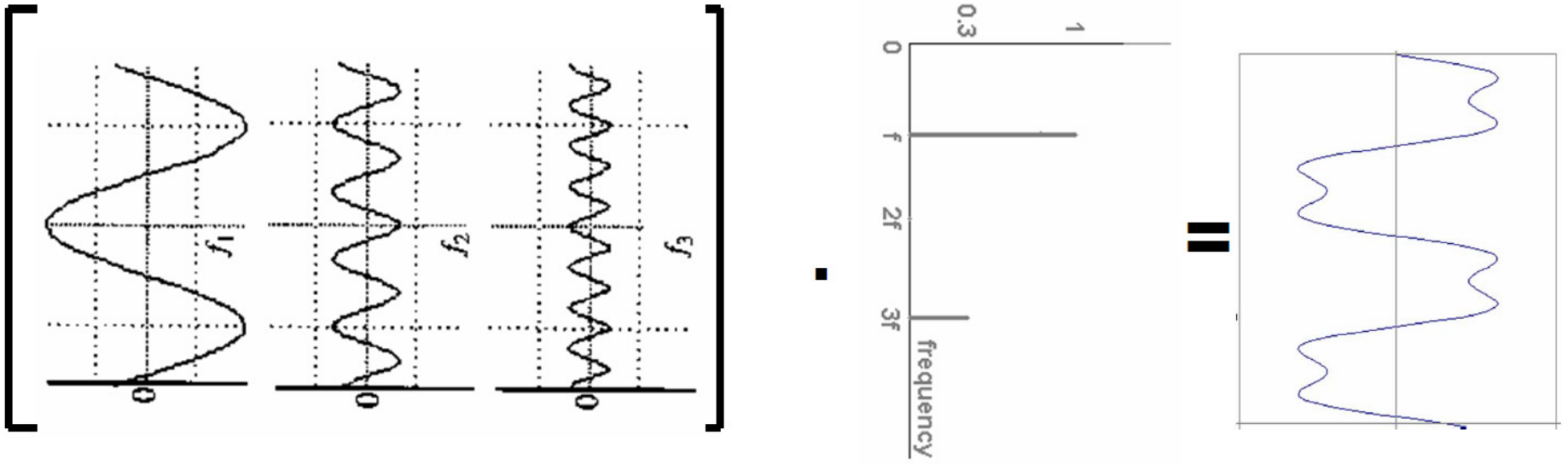

The 2D Fourier Transform

The analysis and synthesis formulas for the 2D continuous Fourier transform are as follows:

Analysis

$$F(u,v) = \int_{-\infty}^{\infty}\int_{-\infty}^{\infty} f(x,y)e^{-j2\pi(ux+vy)}dx\,dy$$

Synthesis

$$f(x,y) = \int_{-\infty}^{\infty}\int_{-\infty}^{\infty} F(u,v)e^{j2\pi(ux+vy)}du\,dv$$

Separability of 2D Fourier Transform

The 2D analysis formula can be written as a 1D analysis in the *x* direction followed by a *1D* analysis in the *y* direction*:*

$$F(u,v) = \int_{-\infty}^{\infty} \left[\int_{-\infty}^{\infty} f(x,y) e^{-j2\pi ux} dx \right] e^{-j2\pi vy} dy$$

The 2D synthesis formula can be written as a 1D synthesis in the *x* direction followed by a 1D synthesis in *y* direction:

$$f(x,y) = \int_{-\infty}^{\infty} \left[\int_{-\infty}^{\infty} F(u,v) e^{j2\pi ux} du \right] e^{j2\pi vy} dv$$

The Discrete Fourier Transform (DFT)

The Discrete Fourier Transform (for sampled signals) can be written as:

$$X[k] = \sum_{n=0}^{N-1} x[n] e^{-j(2\pi/N)kn}.$$

With this notation the DFT Analysis and Synthesis pair becomes:

$$X[k] = \sum_{n=0}^{N-1} x[n] W_N^{kn}$$

$$x[n] = \frac{1}{N} \sum_{k=0}^{N-1} X[k] W_N^{-kn}.$$

Numerical examples

The DFT for N samples can be obtained as the multiplication of the N samples by the W matrix

$$W = W_N^{kn}\Big|_{k,n=0,\ldots,N-1}$$

$$W = \begin{bmatrix} 1 & 1 & 1 & 1 & \cdots & 1 \\ 1 & W_N & W_N^2 & W_N^3 & \cdots & W_N^{N-1} \\ 1 & W_N^2 & W_N^4 & W_N^6 & \cdots & W_N^{2(N-1)} \\ 1 & W_N^3 & W_N^6 & W_N^9 & \cdots & W_N^{3(N-1)} \\ \vdots & \vdots & \vdots & \vdots & & \vdots \\ 1 & W_N^{N-1} & W_N^{2(N-1)} & W_N^{3(N-1)} & \cdots & W_N^{(N-1)(N-1)} \end{bmatrix}$$

DFT examples

N=2

$$W = \begin{bmatrix} 1 & 1 \\ 1 & -1 \end{bmatrix}$$

N=4

$$W = \begin{bmatrix} 1 & 1 & 1 & 1 \\ 1 & -j & -1 & j \\ 1 & -1 & 1 & -1 \\ 1 & j & -1 & -j \end{bmatrix}$$

N=8

$$W = \begin{bmatrix} W_8^0 & W_8^0 & W_8^0 & W_8^0 & \cdots & W_8^0 \\ W_8^0 & W_8^1 & W_8^2 & W_8^3 & \cdots & W_8^7 \\ W_8^0 & W_8^2 & W_8^4 & W_8^6 & \cdots & W_8^{14} \\ W_8^0 & W_8^3 & W_8^6 & W_8^9 & \cdots & W_8^{21} \\ \vdots & \vdots & \vdots & \vdots & \ddots & \vdots \\ W_8^0 & W_8^7 & W_8^{14} & W_8^{21} & \cdots & W_8^{49} \end{bmatrix}$$

$$W_8 = e^{-j\frac{2\pi}{8}} =$$

$$= \frac{1}{\sqrt{2}} - \frac{j}{\sqrt{2}}$$

DFT for N=8

The DFT for N samples seen as the projection on N complex exponential sequences

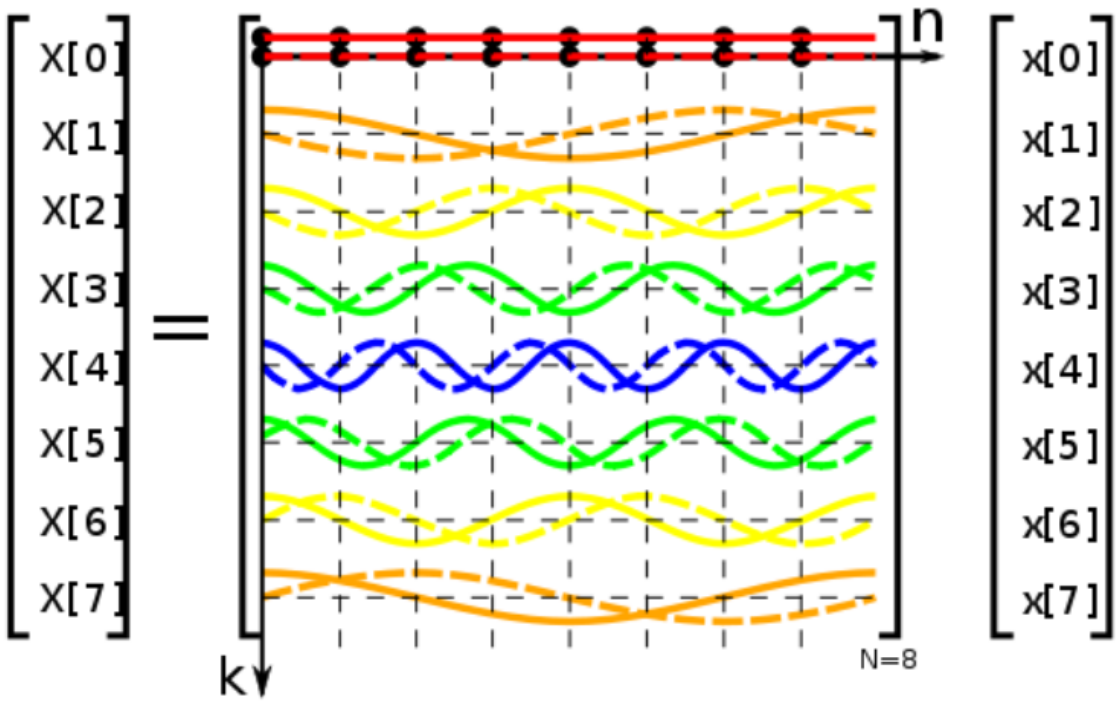

Example

Consider a periodic signal whose period is [0 1 2 3]

If we want to get the DFT of the input signal we can write:

$$X = \begin{bmatrix} 1 & 1 & 1 & 1 \\ 1 & -j & -1 & j \\ 1 & -1 & 1 & -1 \\ 1 & j & -1 & -j \end{bmatrix} \begin{bmatrix} 0 \\ 1 \\ 2 \\ 3 \end{bmatrix} = \begin{bmatrix} 6 \\ -2+2j \\ -2 \\ -2-2j \end{bmatrix}$$

Inverse DFT

The inverse of the W matrix will be equal to its conjugate transpose divided by N, for example for N=4

$$W^{-1} = \frac{1}{4}\begin{bmatrix} 1 & 1 & 1 & 1 \\ 1 & j & -1 & -j \\ 1 & -1 & 1 & -1 \\ 1 & -j & -1 & j \end{bmatrix}$$

The iDFT for the previous example will then be:

$$y = \frac{1}{4}\begin{bmatrix} 1 & 1 & 1 & 1 \\ 1 & j & -1 & -j \\ 1 & -1 & 1 & -1 \\ 1 & -j & -1 & j \end{bmatrix}\begin{bmatrix} 6 \\ -2-2j \\ -2 \\ -2-2j \end{bmatrix} = \begin{bmatrix} 0 \\ 1 \\ 2 \\ 3 \end{bmatrix}$$

Sinusoidal waves

The 2D Fourier Transform is based on a decomposition into complex functions:

$$e^{j2\pi(ux+vy)} = \cos 2\pi(ux+vy) + j\sin 2\pi(ux+vy)$$

The real and imaginary terms are sinusoids on the *x,y* plane.

Sinusoidal waves

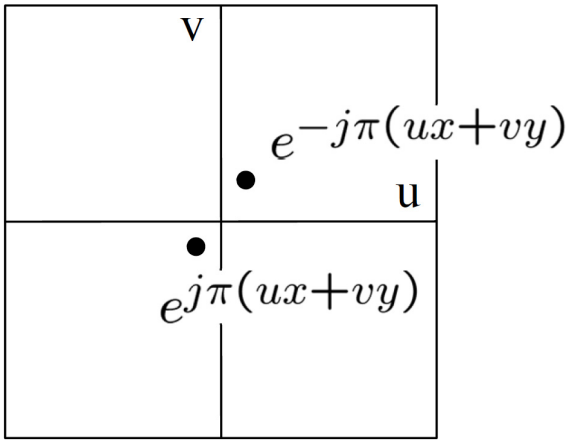

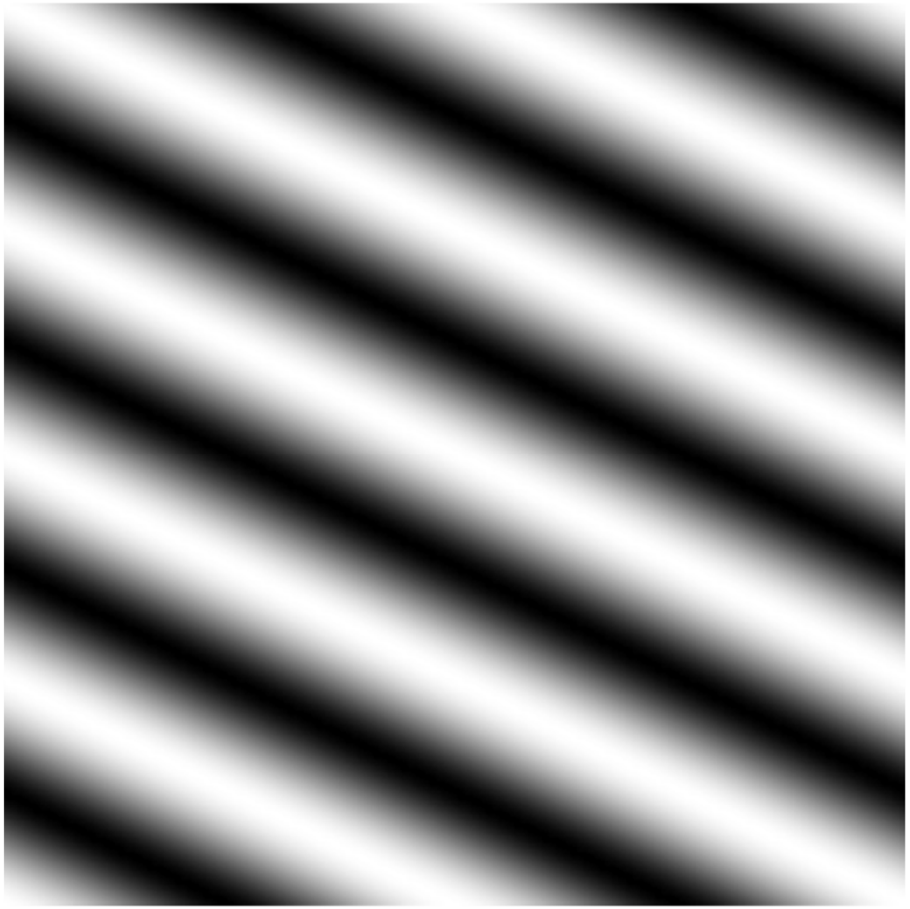

Sinusoidal waves

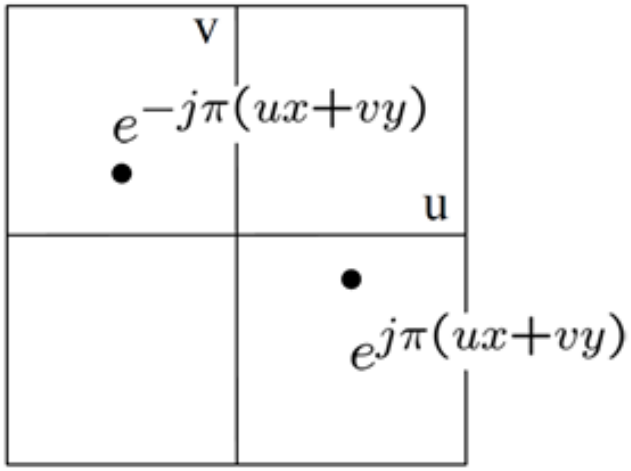

Sinusoidal waves

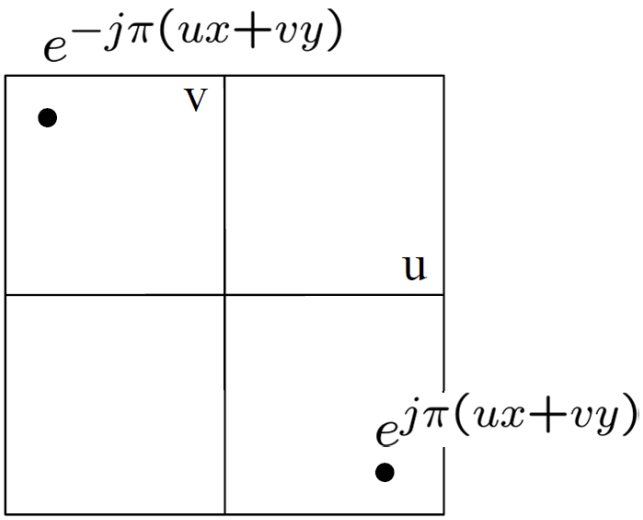

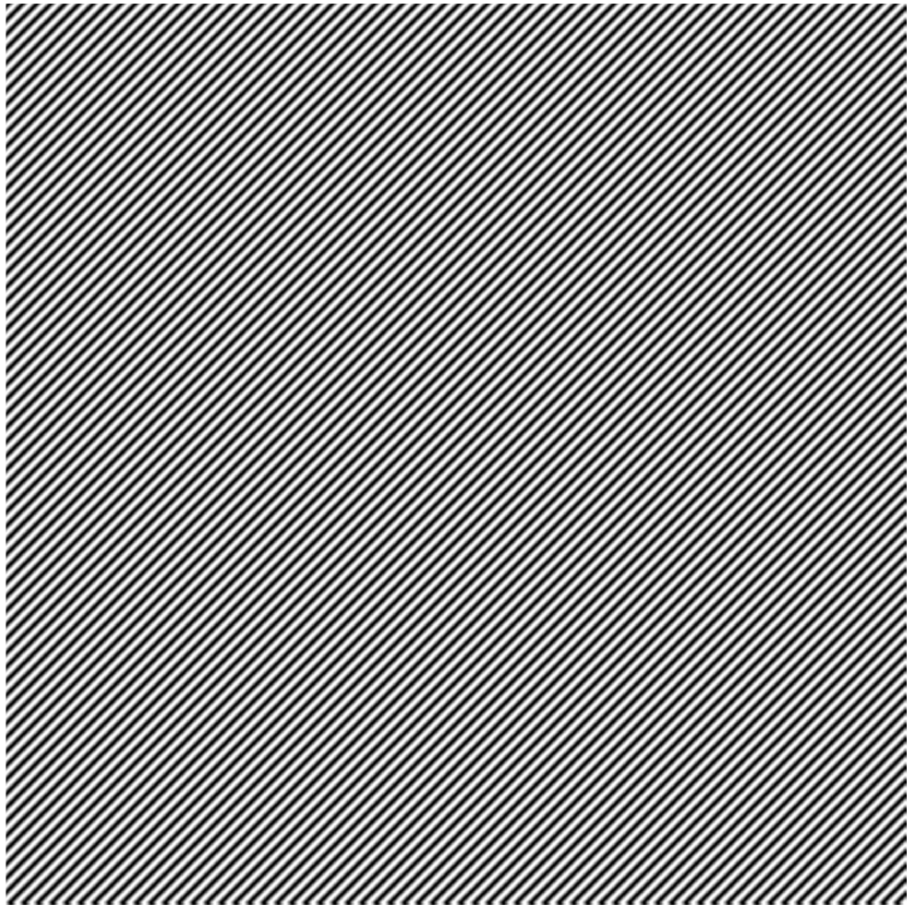

Fourier Transform Pair example

$$
\begin{aligned}
F(u,v) &= \int\int f(x,y)e^{-j2\pi(ux+vy)}dxdy, \\
&= \int_{-X/2}^{X/2} e^{-j2\pi ux}dx \int_{-Y/2}^{Y/2} e^{-j2\pi vy}dy, \\
&= \left[\frac{e^{-j2\pi ux}}{-j2\pi u}\right]_{-X/2}^{X/2} \left[\frac{e^{-j2\pi vy}}{-j2\pi v}\right]_{-Y/2}^{Y/2}, \\
&= \frac{1}{-j2\pi u}\left[e^{-juX} - e^{juX}\right]\frac{1}{-j2\pi v}\left[e^{-jvY} - e^{jvY}\right], \\
&= XY\left[\frac{sin(\pi Xu)}{\pi Xu}\right]\left[\frac{sin(2\pi Yv)}{\pi Yv}\right] \\
&= XY\mathrm{sinc}(\pi \mathrm{Xu})\mathrm{sinc}(\pi \mathrm{Yv}).
\end{aligned}
$$

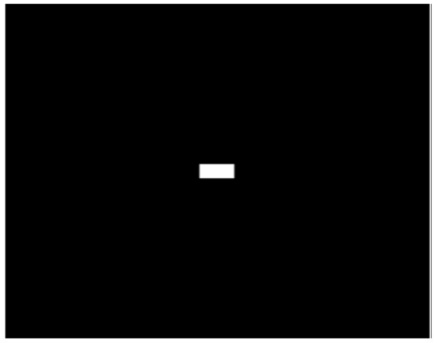

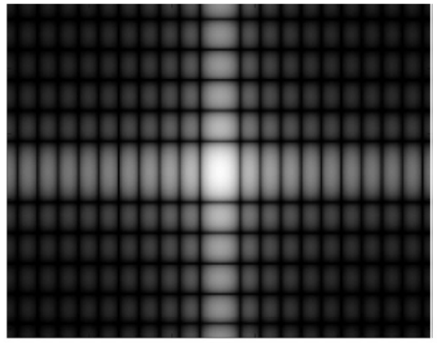

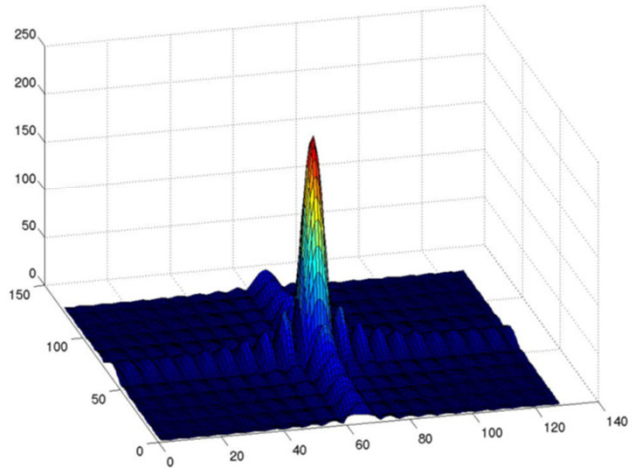

The 2D Discrete Fourier Transform for periodic signals

The analysis and synthesis formulas for the 2D discrete Fourier transform are as follows:

Analysis

$$\hat{F}(k,\ell) = \frac{1}{\sqrt{MN}} \sum_{m=0}^{M-1} \sum_{n=0}^{N-1} F(m,n) e^{-j2\pi\left(k\frac{m}{M}+\ell\frac{n}{N}\right)}$$

Synthesis

$$F(m,n) = \frac{1}{\sqrt{MN}} \sum_{k=0}^{M-1} \sum_{\ell=0}^{N-1} \hat{F}(k,\ell) e^{j2\pi\left(k\frac{m}{M}+\ell\frac{n}{N}\right)}$$

Separability of 2D Discrete Fourier Transform

$$\hat{F}(k,\ell) = \frac{1}{\sqrt{N}} \sum_{n=0}^{N-1} \left[\frac{1}{\sqrt{M}} \sum_{m=0}^{M-1} F(m,n) e^{-j2\pi\left(k\frac{m}{M}\right)} \right] e^{-j2\pi\left(\ell\frac{n}{N}\right)}$$

The 2D forward DFT (for a squared input matrix of size SxS) can be written in matrix notation:

$$\hat{\mathbf{F}} = (\mathbf{W}^{*}\mathbf{F})\,\mathbf{W}^{*}$$

Where *r* and *c* are row and column indexes starting from zero.

$$W_{rc}^{*} = \frac{1}{\sqrt{S}} e^{-j2\pi\frac{rc}{S}}$$

Separability of 2D Discrete Fourier Transform

And

$$F(m,n) = \frac{1}{\sqrt{N}} \sum_{\ell=0}^{N-1} \left[\frac{1}{\sqrt{M}} \sum_{k=0}^{M-1} \hat{F}(k,\ell) e^{j2\pi\left(k\frac{m}{M}\right)} \right] e^{j2\pi\left(\ell\frac{n}{N}\right)}.$$

The 2D inverse DFT can be written in matrix notation:

$$\mathbf{F} = \left(\mathbf{W}\hat{\mathbf{F}}\right)\mathbf{W}$$

Where the matrix elements are

$$W_{rc} = \frac{1}{\sqrt{A}} e^{j2\pi\frac{rc}{A}}$$

Transform examples

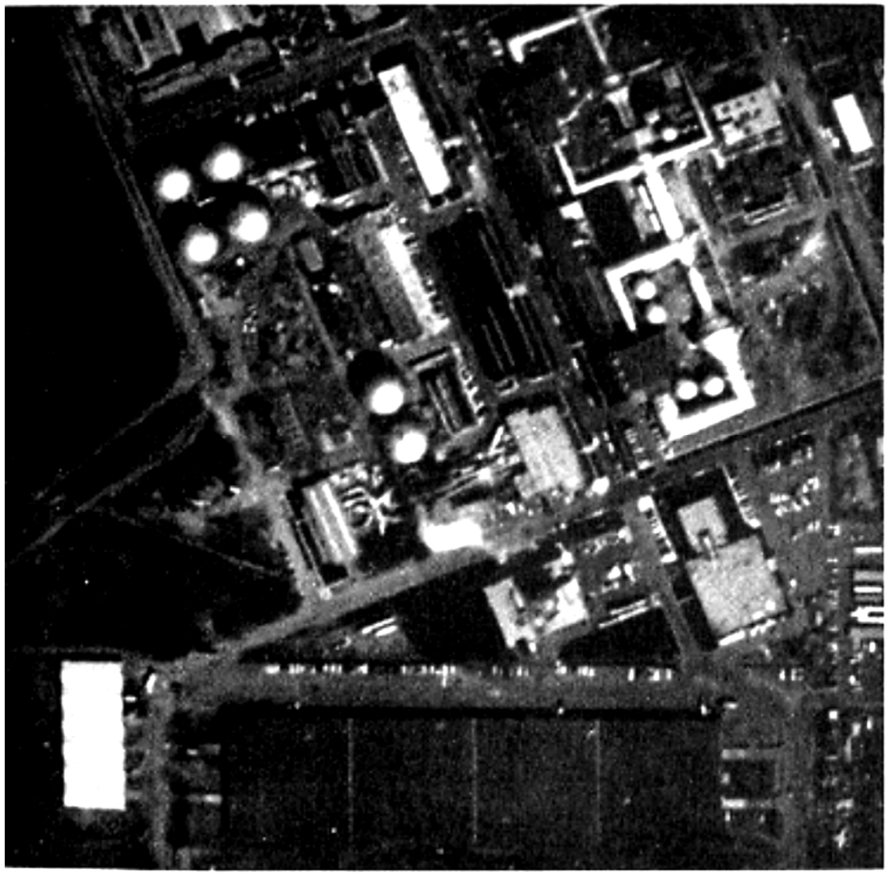

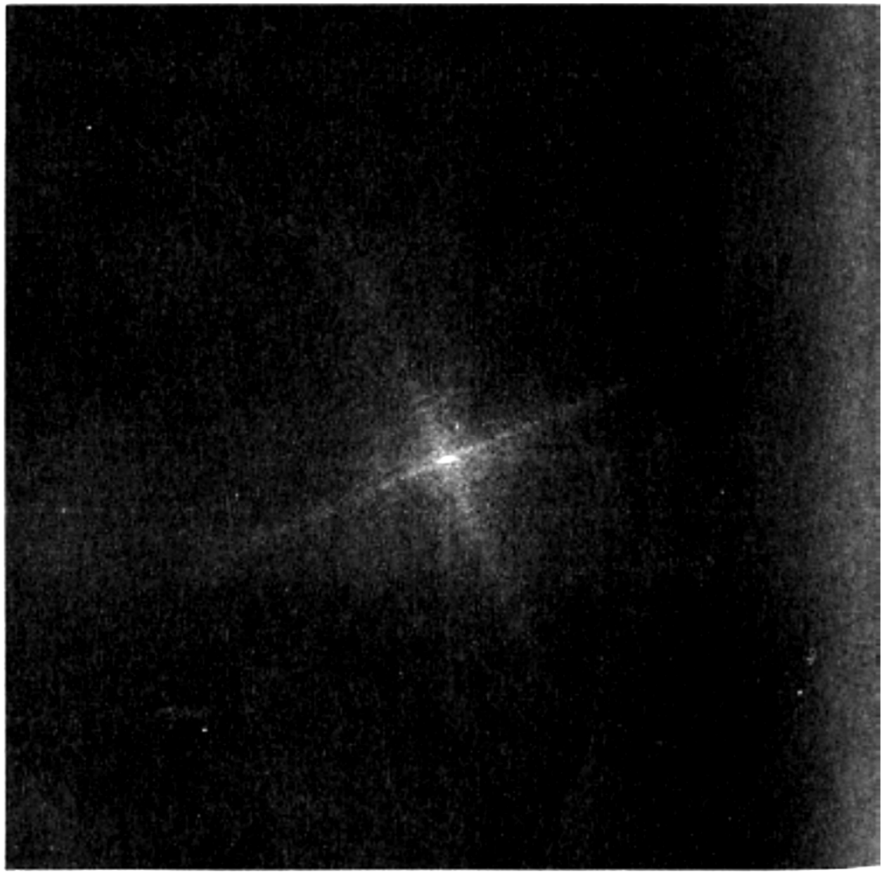

2D DFT Example

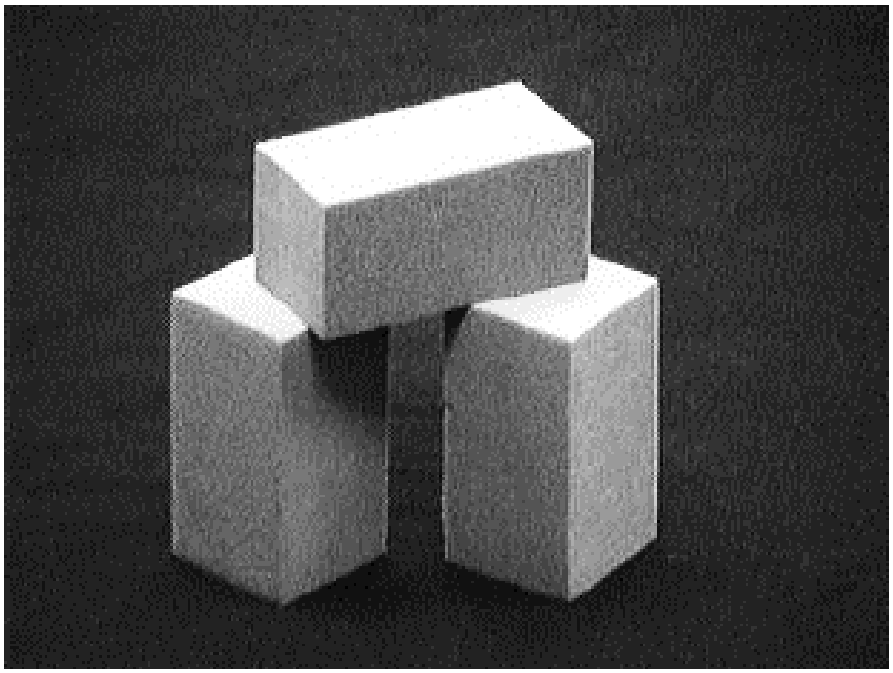

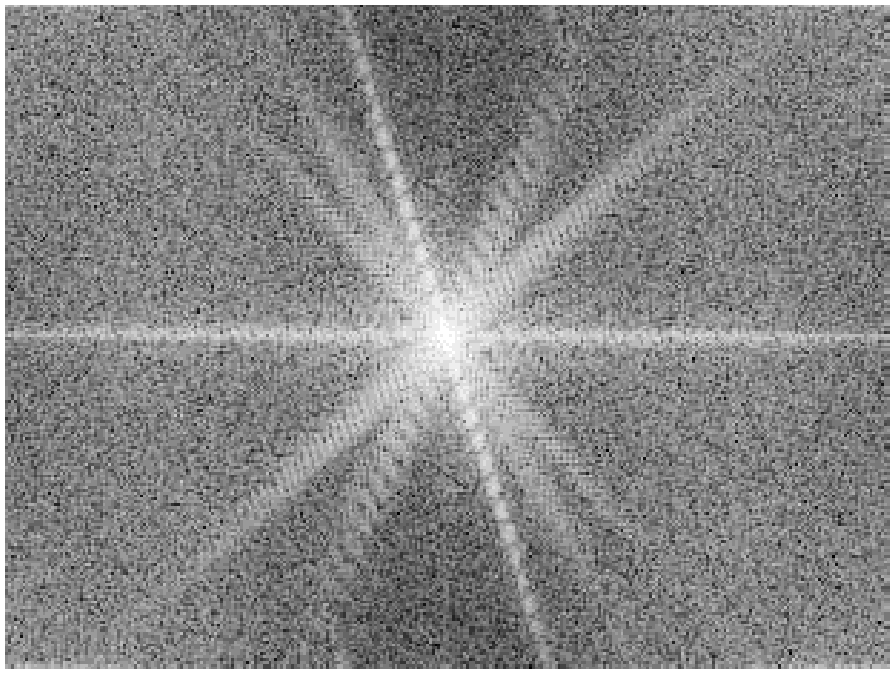

low-pass (blurred) version of an image

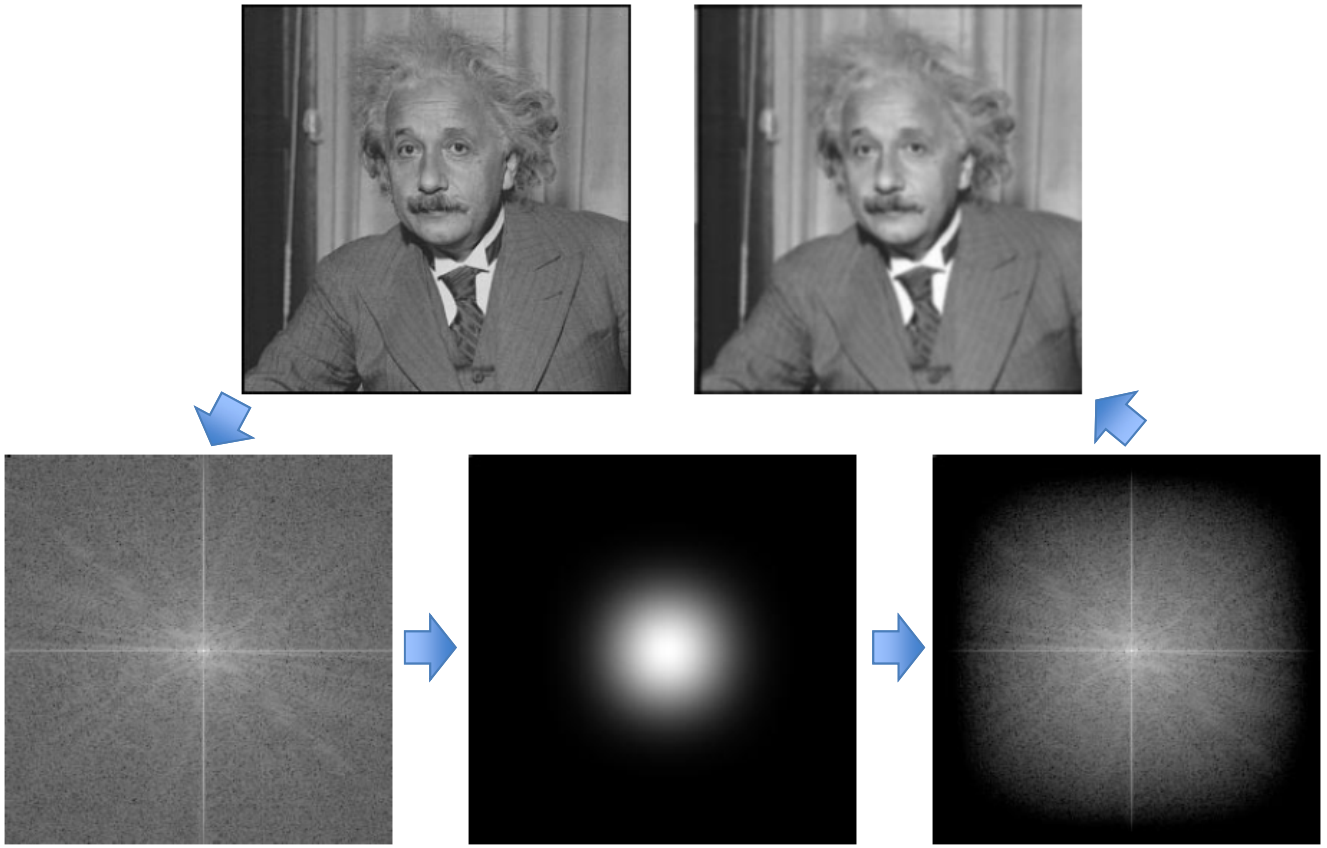

Hi-Pass Filter

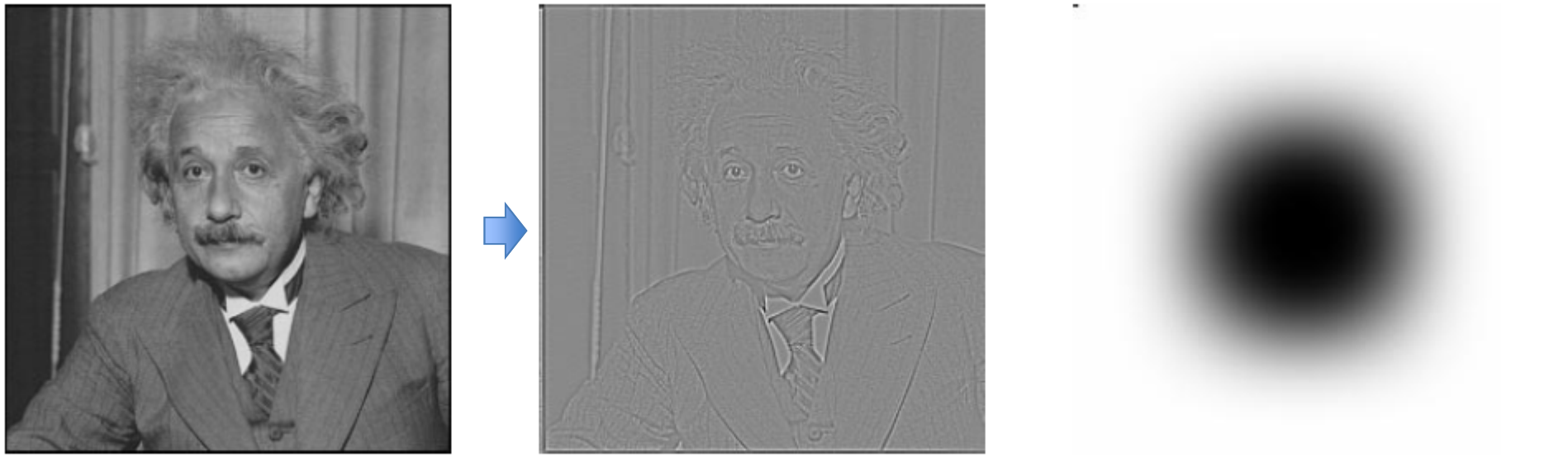

a high-pass filtered version of Albert, and the amplitude spectrum of the filter. This impulse response is defined by $\delta(n)$-$h(n,m)$ where $h(n,m)$ is the separable blurring kernel used in the previous figure

Band Pass Filter

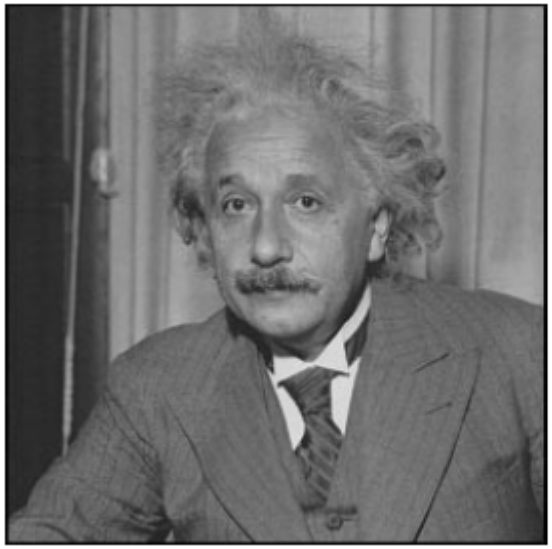

a band-pass filtered version of Albert, and the amplitude spectrum of the filter.

This impulse response is defined by the difference of two low-pass filters.

Directional filters

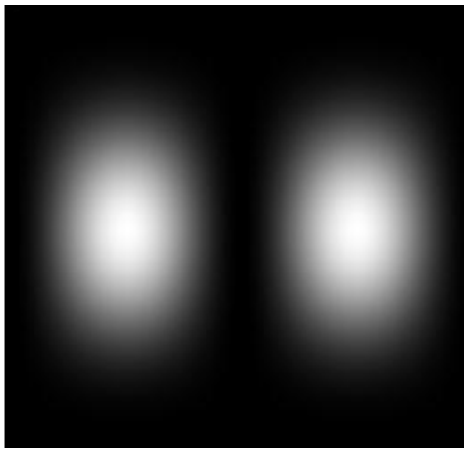

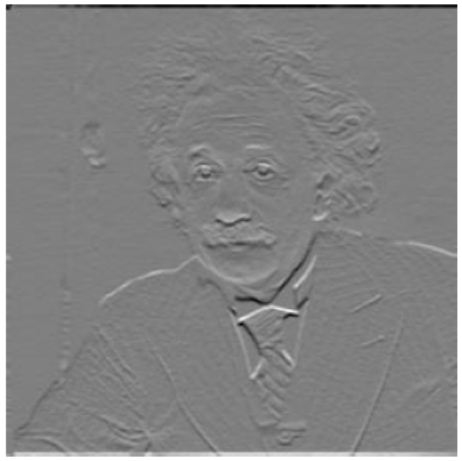

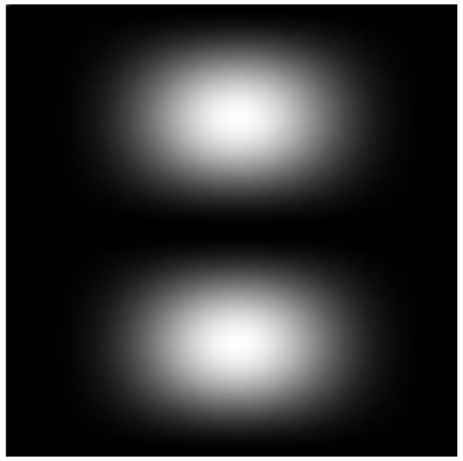

Goal: recognize lines in images

Approach:

- For every point in the starting image plot the sinusoid on the dual plane (parameter space): (ρ, ϑ)

  $\rho = x^*\cos(\vartheta) + y^*\sin(\vartheta)$

  where x and y are fixed (the considered point coordinates) while ρ and ϑ are variables.
- The Hough Transform of an image with K lines is the sum of many sinusoids intersecting in K points.
- Maxima in the dual plane indicate the parameters of the k lines

Hough: implementation

Consider a discretization of the dual plane for the parameters (ρ,ϑ): it becomes a matrix whose raw and column indices correspond to the quantized values of ρ and ϑ.

The limits of ρ are chosen accordingly to the image size.

Usually: $-\rho_{max} \leq \rho \leq \rho_{max}$, $-\pi/2 \leq \vartheta \leq \pi/2$

Hough: implementazion

Clear the matrix H(m,n);

Fro every point P(x,y) of the image

- 1. for ϑ_n that ranges from -π/2 to π/2 with step dϑ
  - 1. Evaluate ρ(n)=x*cos(ϑ_n)+y*sin(ϑ_n)
  - 2. find the index *m* corresponding to *ρ(n)*
  - 3. Increase H(m,n)
- 2. end

end

4. Find local maxima in H(.,.) that will corresponds to parameters of the founded lines

Hough Trasform

5 points

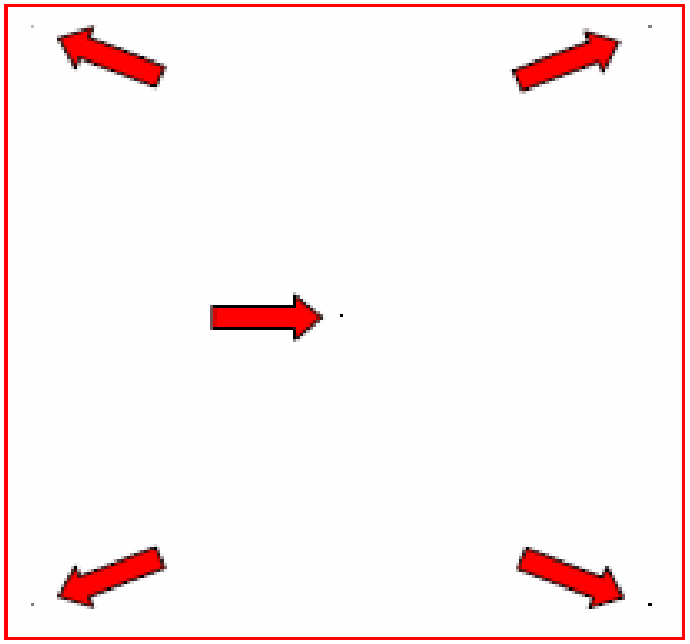

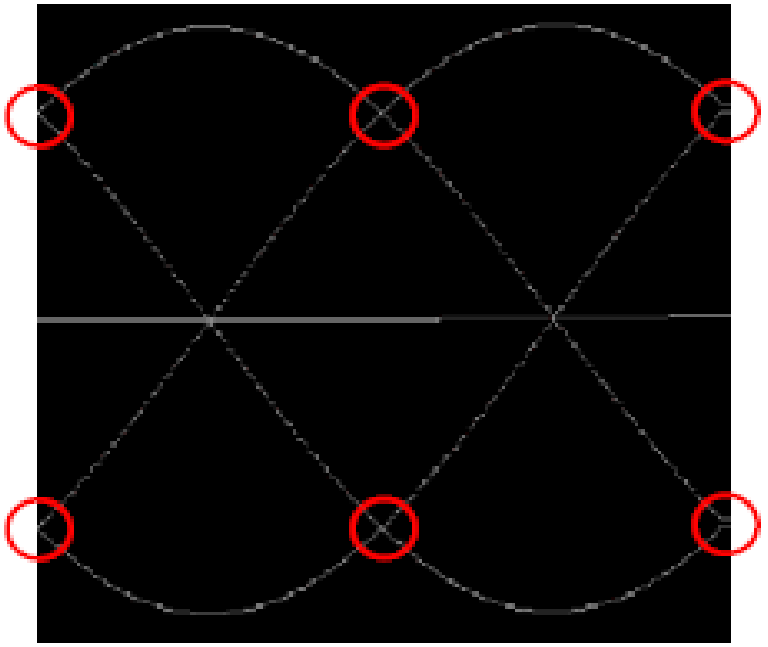

Hough Trasform

line $\rho>0,\theta>0$

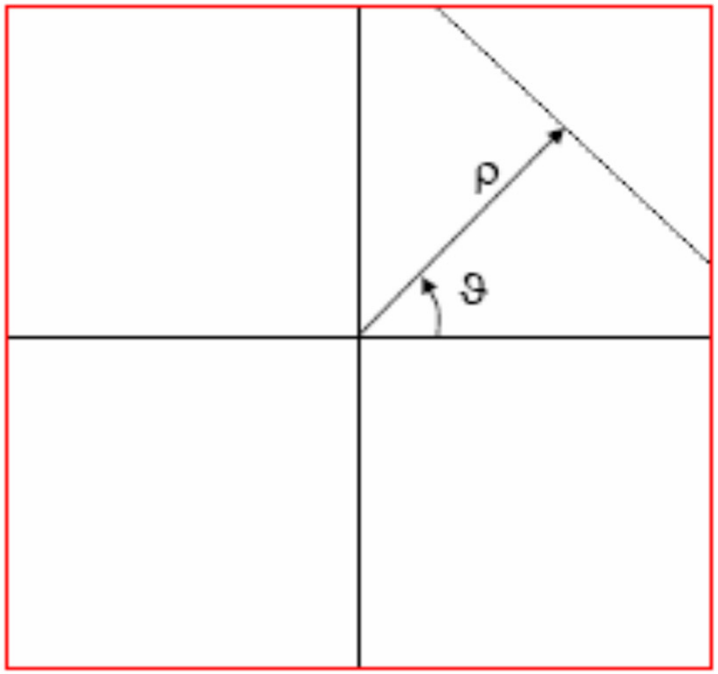

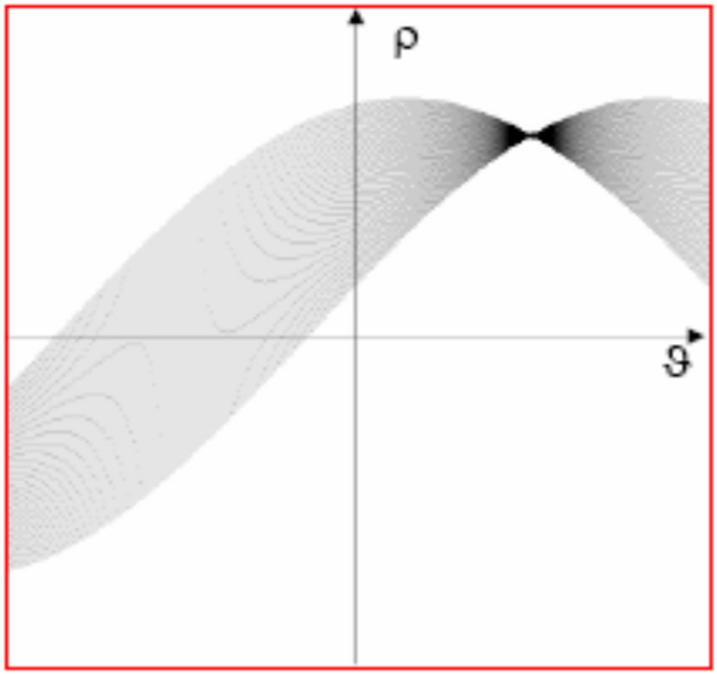

Hough Trasform

line $\rho>0,\theta<0$

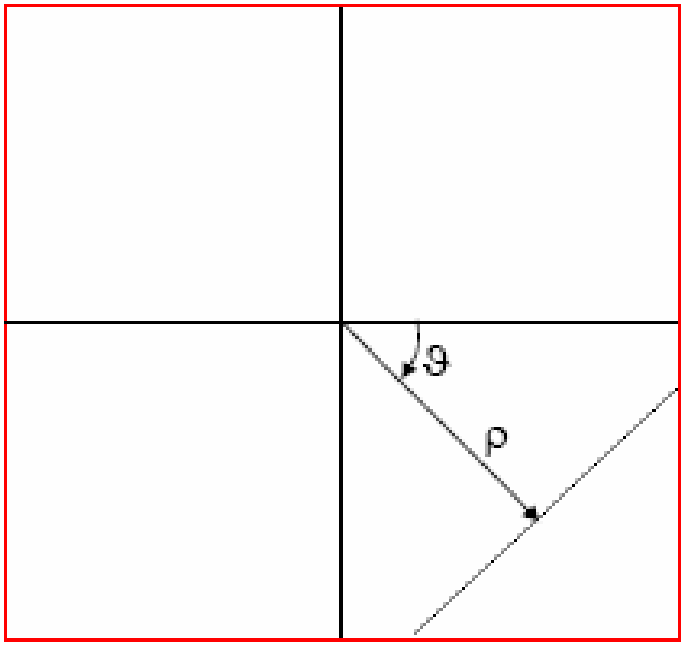

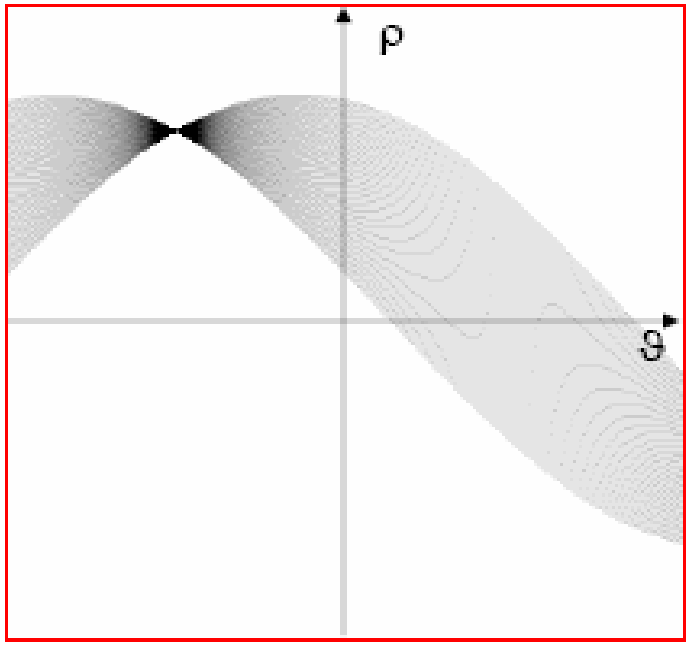

Hough Trasform

line $\rho<0,\theta>0$

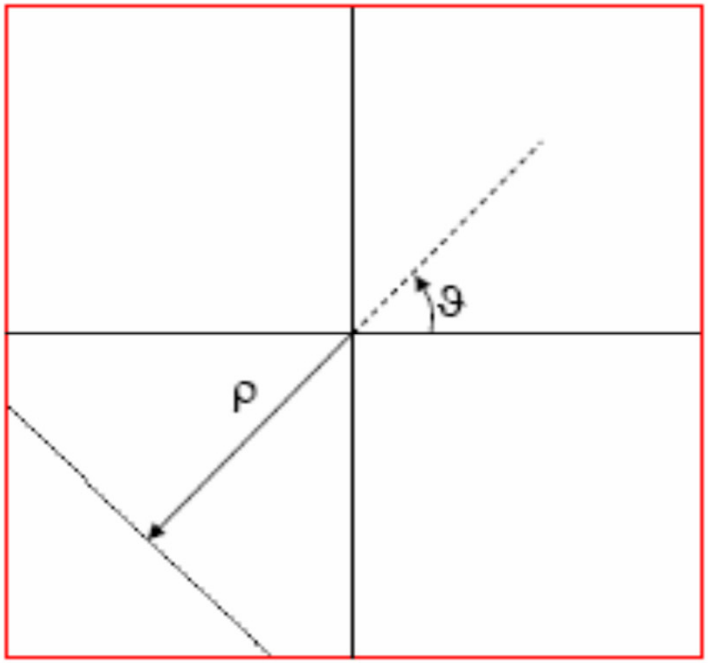

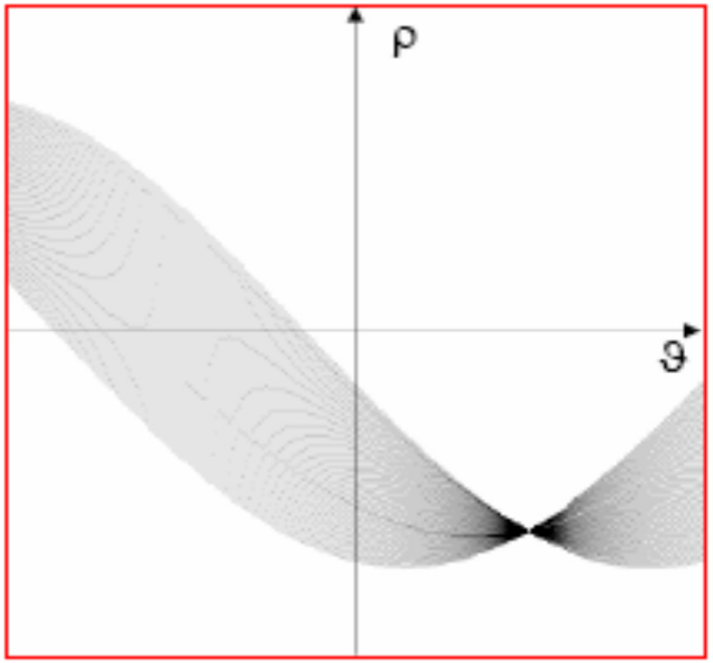

Hough Trasform

Dotted line

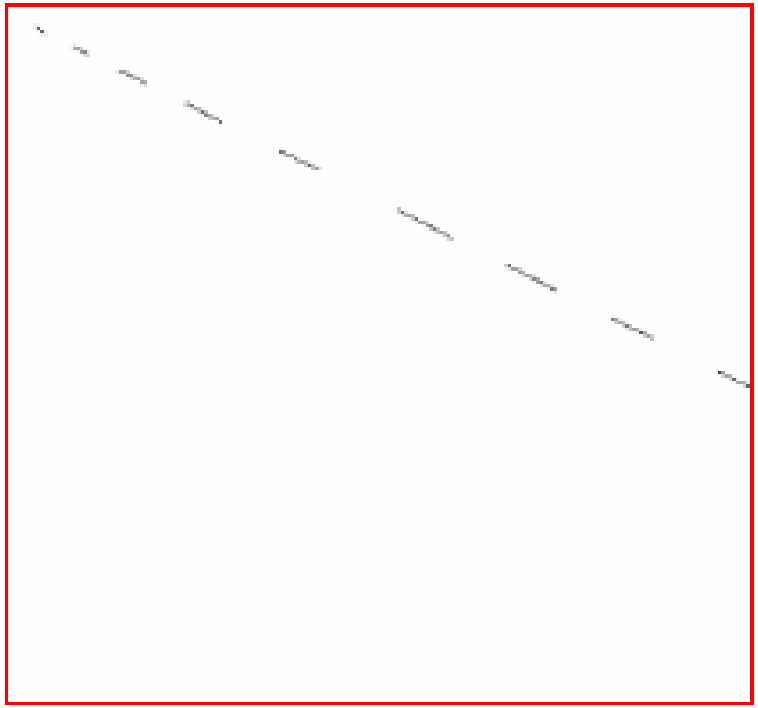

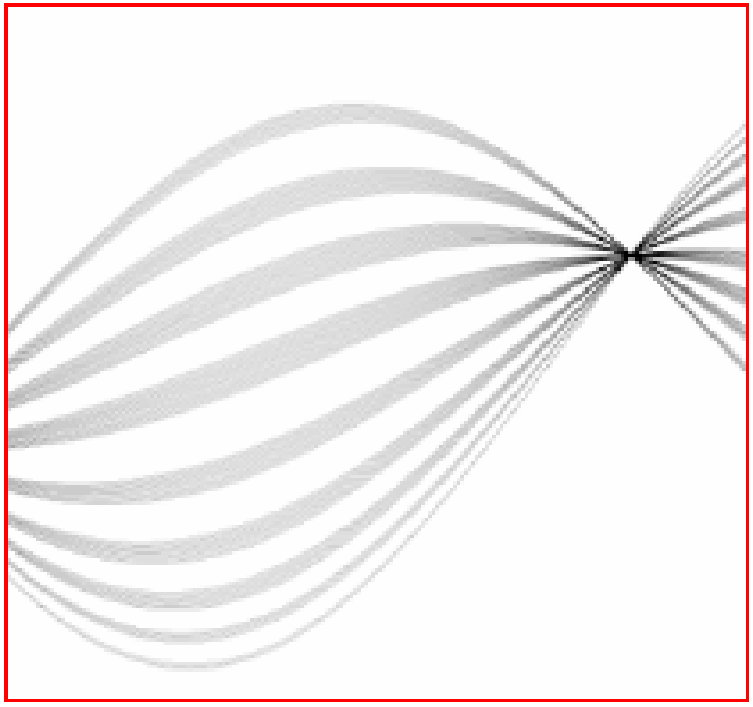

Hough Trasform

Same text with different orientations

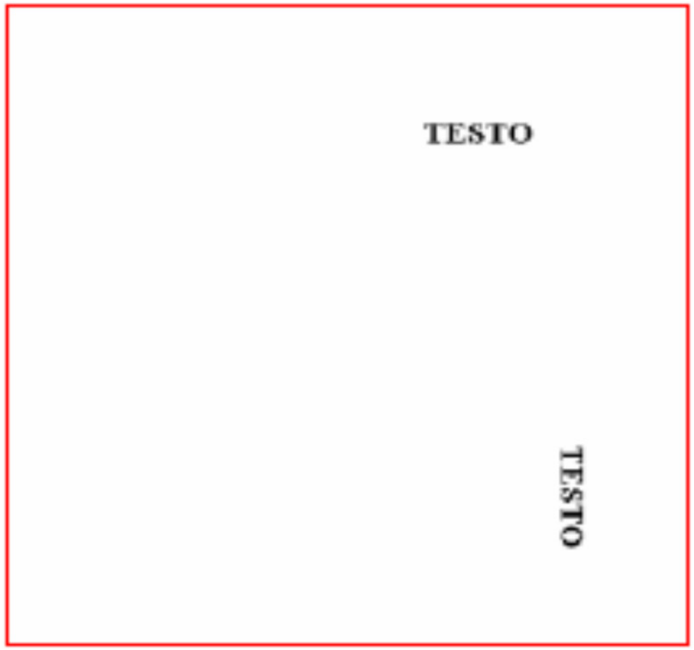

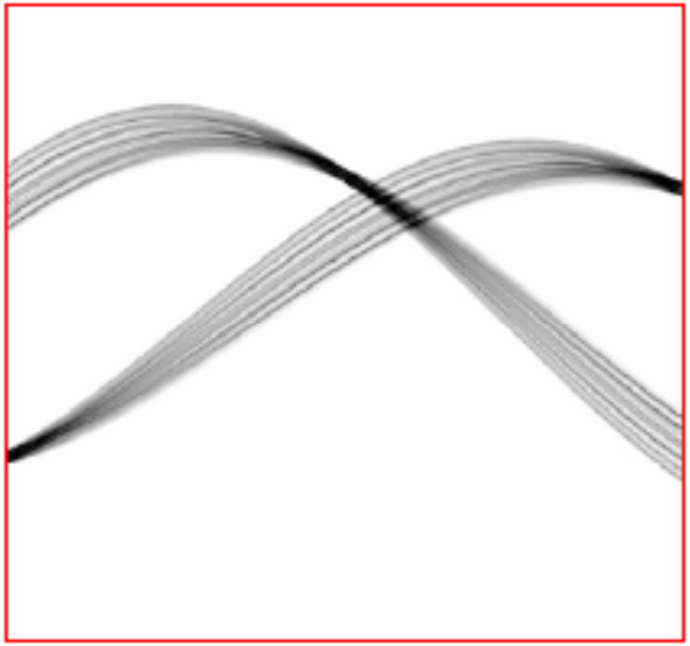

Hough Trasform

Noisy and noiseless square

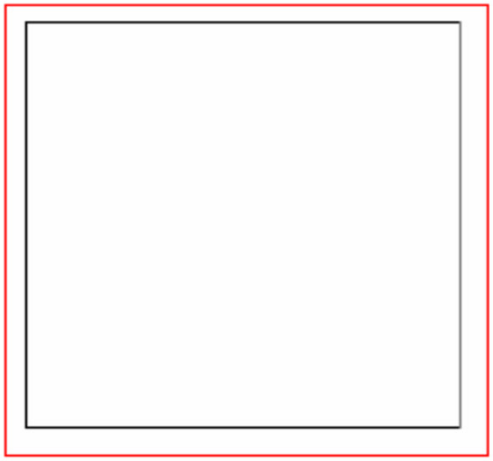

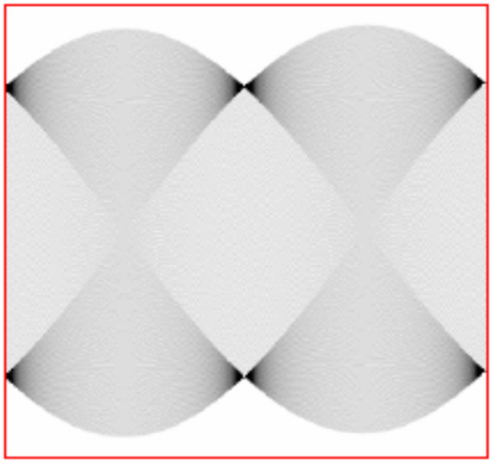

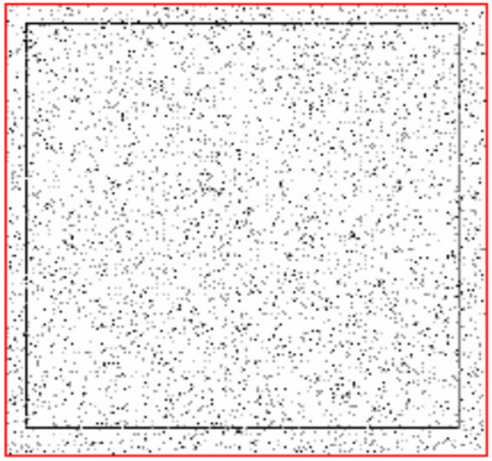

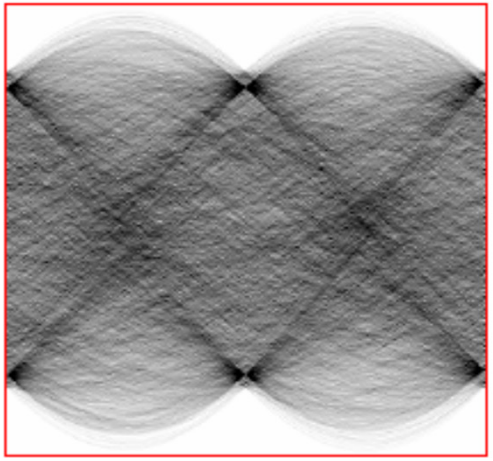

Hough Trasform

Accumulation matrices of the previous images

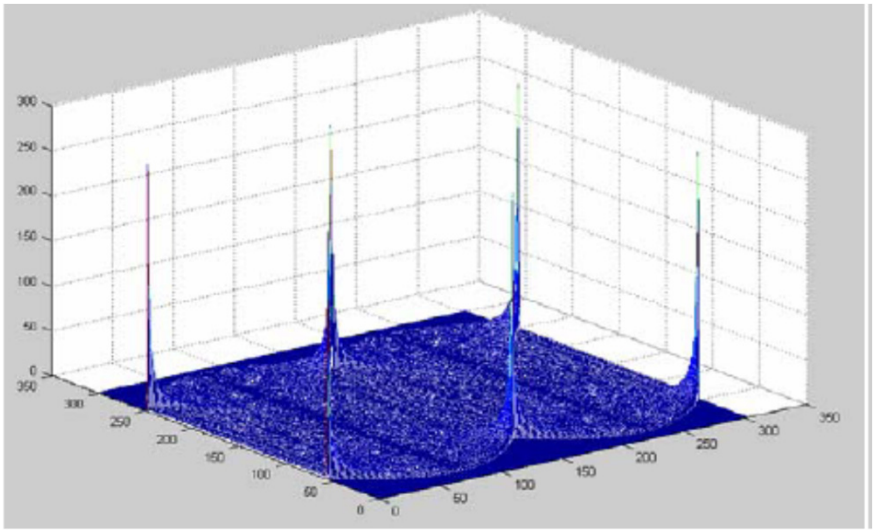

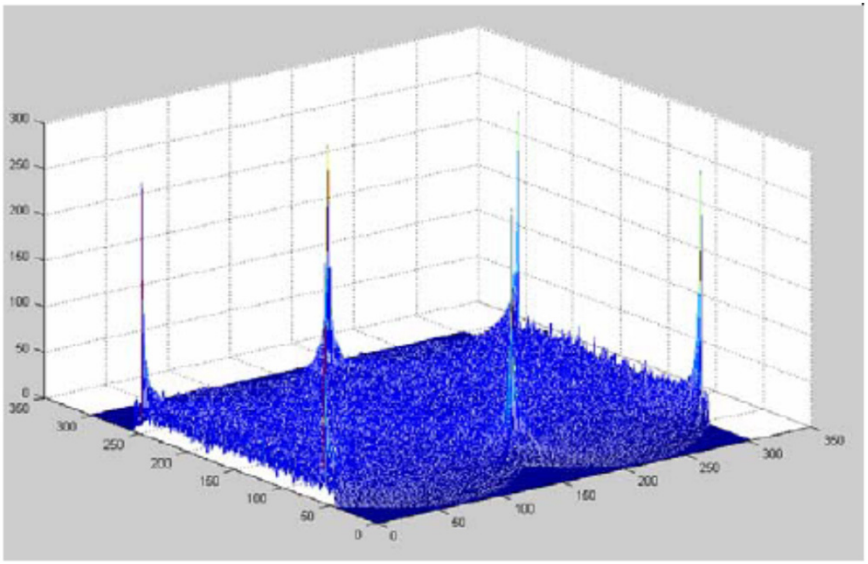

Examples

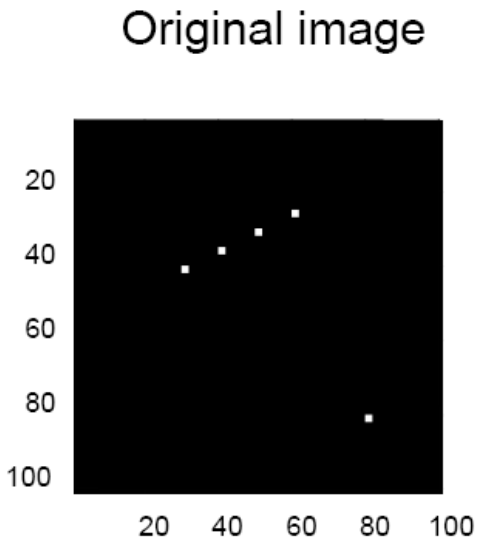

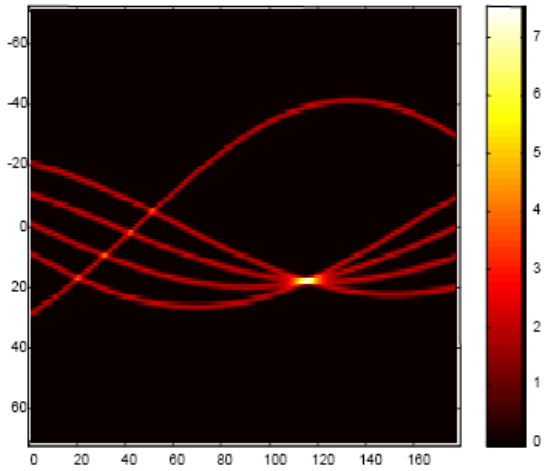

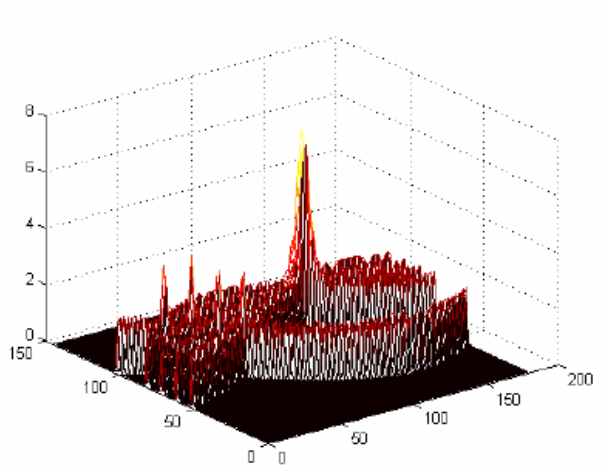

Courtesy: P. Salembier

Example

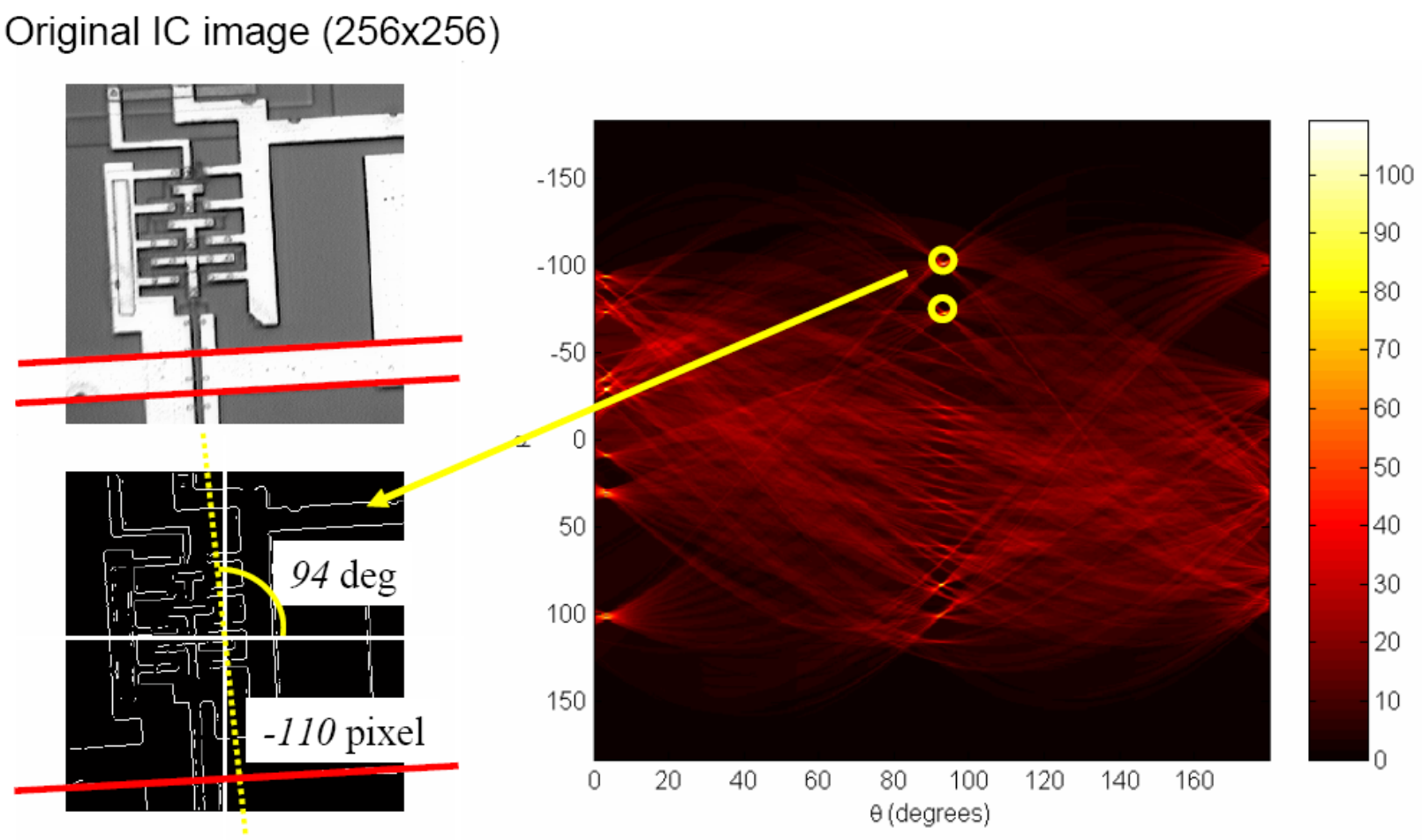
Original IC image (256x256)
94 deg
-110 pixel
-150
-100
-50
0
50
100
150
0
20
40
60
80
100
120
140
160
θ (degrees)
100
90
80
70
60
50
40
30
20
10
0

Radon and Hough transforms

The Hough transform and the Radon transform are indeed very similar to each other and their relation can be loosely defined as the former being a discretized form of the latter.

The Radon transform is a mathematical integral transform, defined on for continuous functions.

The Hough transform, on the other hand, is inherently a discrete algorithm that detects lines (extendable to other shapes) in an image by polling and binning (or voting).

The Beer-Lambert Law

The Beer-Lambert law connects the initial (known) and final (measured) intensities of an X-ray:

$$I(s) = I_0 \exp\left(-\int_l \mu_a(s)\,ds\right) \rightarrow \int_l \mu_a(s)\,ds = -\log\left(\frac{I_L}{I_0}\right)$$

$$\begin{cases} \dfrac{dI}{ds} = -\mu_a I & \mu_a = \mu_a(s) \\ I(s=0) = I_0 & \textit{source} \\ I(s=L) = I_L & \textit{detector} \end{cases}$$

We only possess line integrals of the quantity of interest

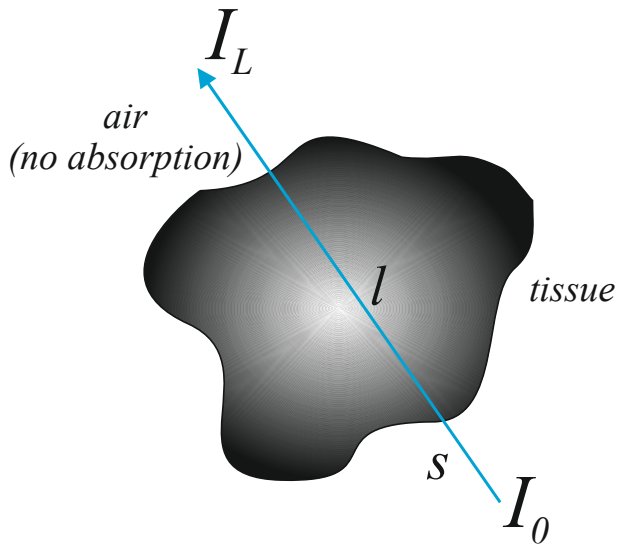

Beer-Lambert law and Radon transform

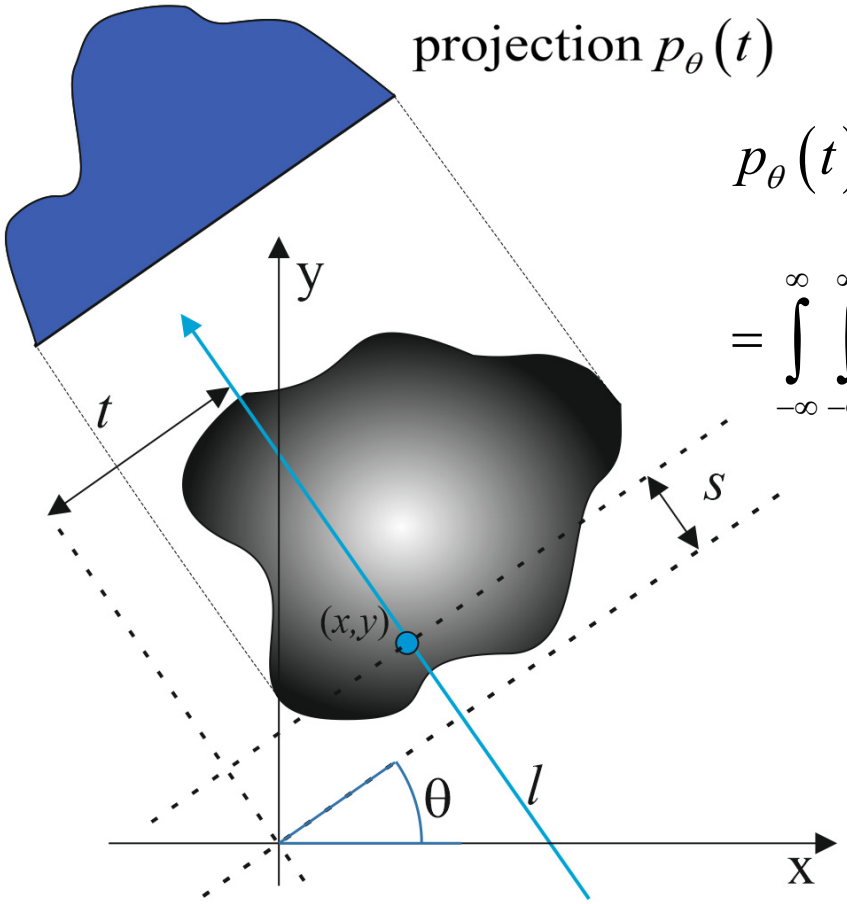

$$p_\theta(t) = \int_l f(x,y)\,ds =$$

$$= \int_{-\infty}^{\infty}\int_{-\infty}^{\infty} f(x,y)\,\delta\left(x\cos(\theta) + y\sin(\theta) - t\right)dxdy$$

$$\int_l \mu_a(s)\,ds = -\log\left(\frac{I_L}{I_0}\right)$$

Hounsfield units

The energy of the X-ray is attenuated from the tissue that it crosses.

The denser the tissue region, the higher the attenuation.

We are interested in a parameter called **absorption** (=attenuation) **coefficient** μ_a.

The result is expressed in relative Hounsfield units:

$$HU = \frac{\mu_a - \mu_{a,H_2O}}{\mu_{a,H_2O} - \mu_{air}} \times 1000$$

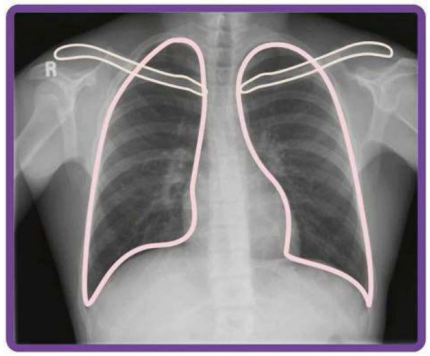

material	HU
water	0
air	-1000
bone	1086
blood	53
muscle	41

CT scan [1972 Cormack, Hounsfield - Nobel Prize 1979]

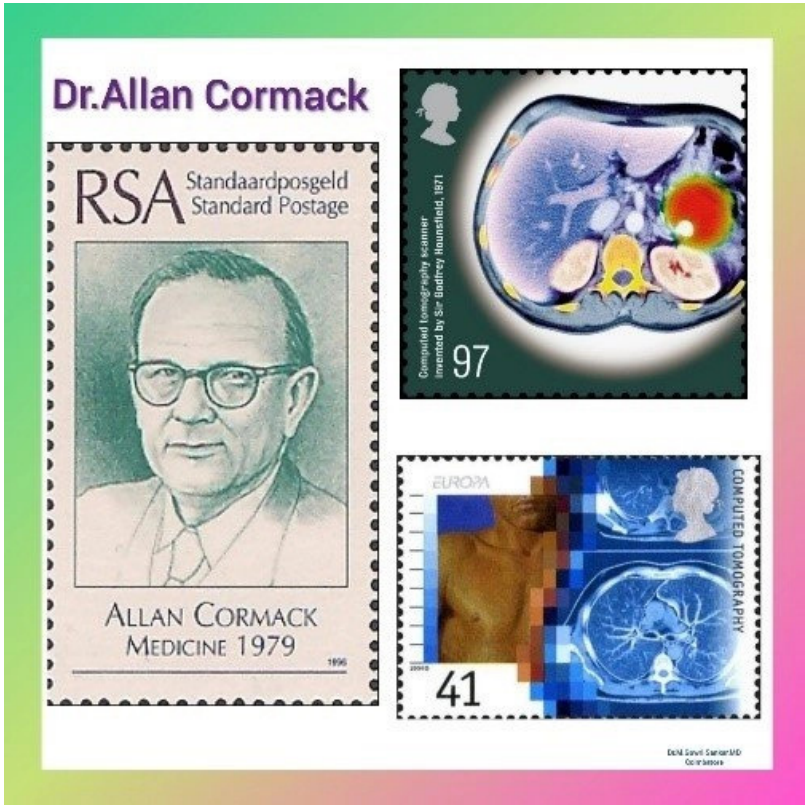

The sinogram

For every angle we obtain a projection, a collection of projections is called sonogram.

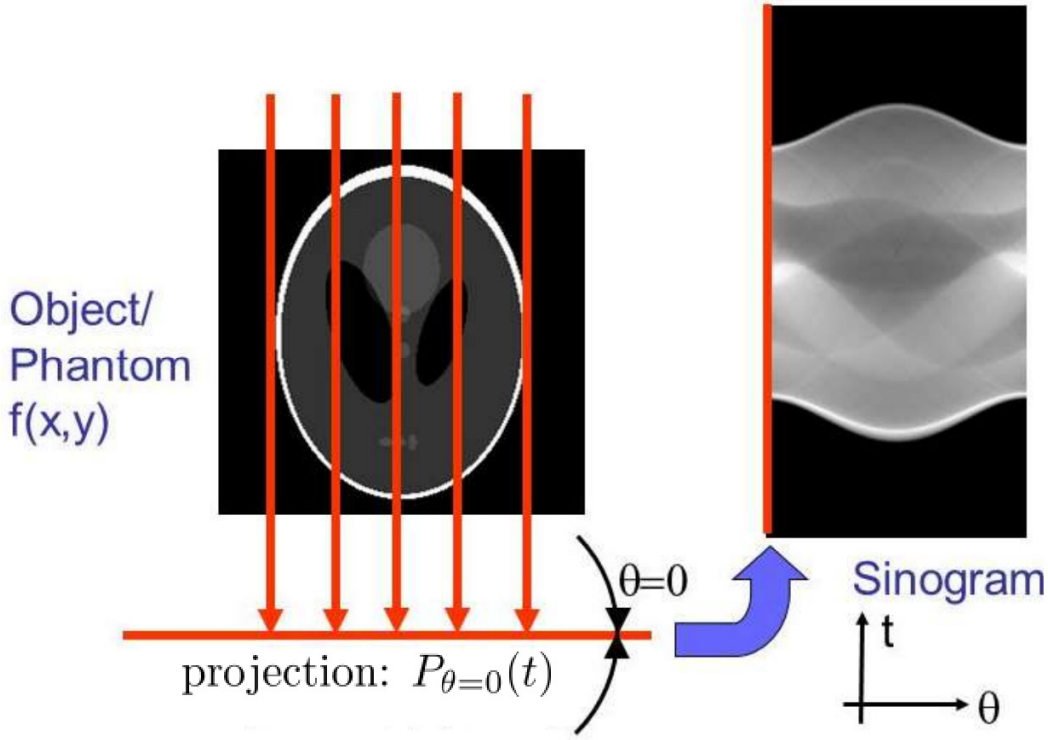

‘Computational’ version

- Sinogram (measured data): already discrete (finite set of angles, finite set of detectors)
- Sample: discretize in voxels
- Various approaches to discretize (compute or approximate) the line integrals

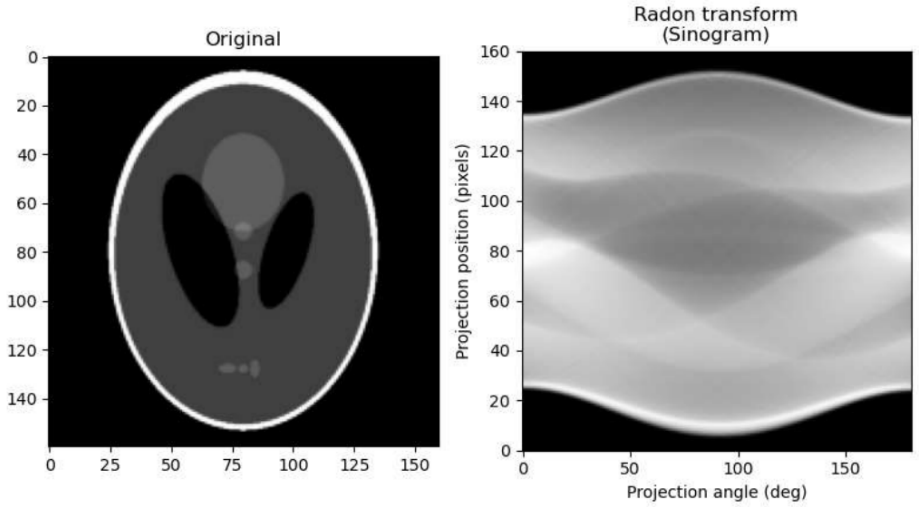

$$\int_{\mathbb{R}^2} \underbrace{\delta(x\cos(\theta)+y\sin(\theta)-t)}_{\mathbf{K}(x,y;\theta,t)} f(x,y)\,dxdy = \mathbf{y}(\theta,t)$$

$$\mathbf{Kf} = \mathbf{y}$$

History of clinical CT scanners

Hounsfield's first generation CT scanner showing the translation-rotation system.

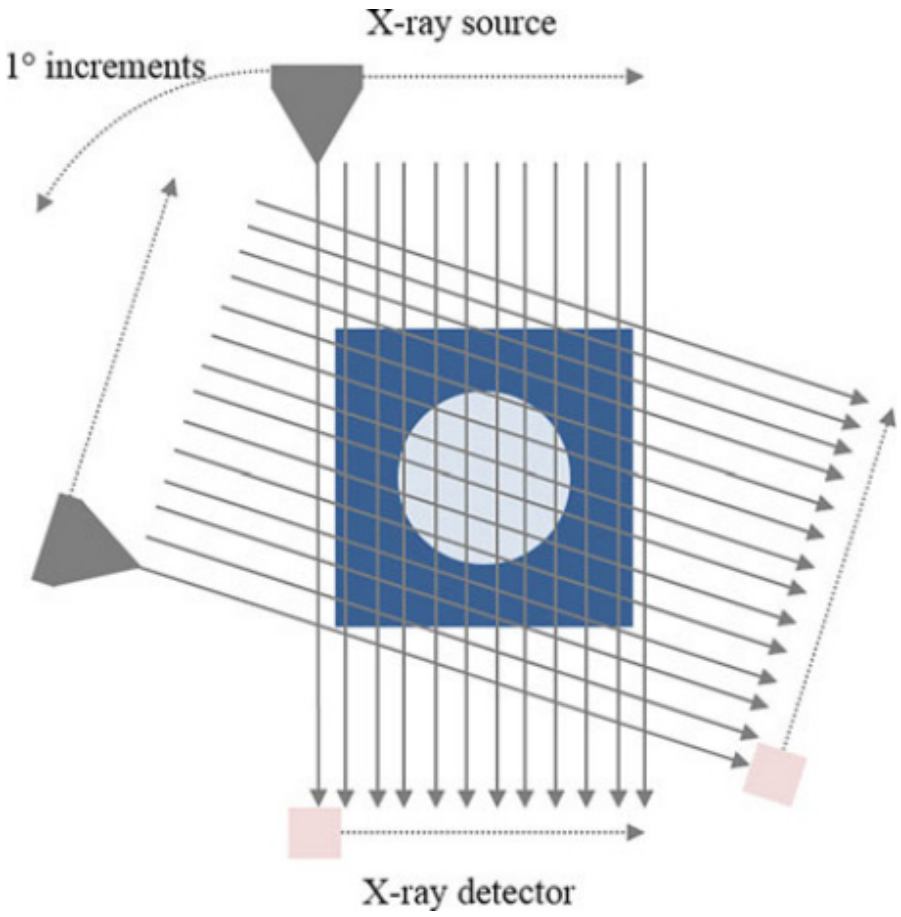

History of clinical CT scanners

The second generation CT scanner, showing the improved translation-rotation system.

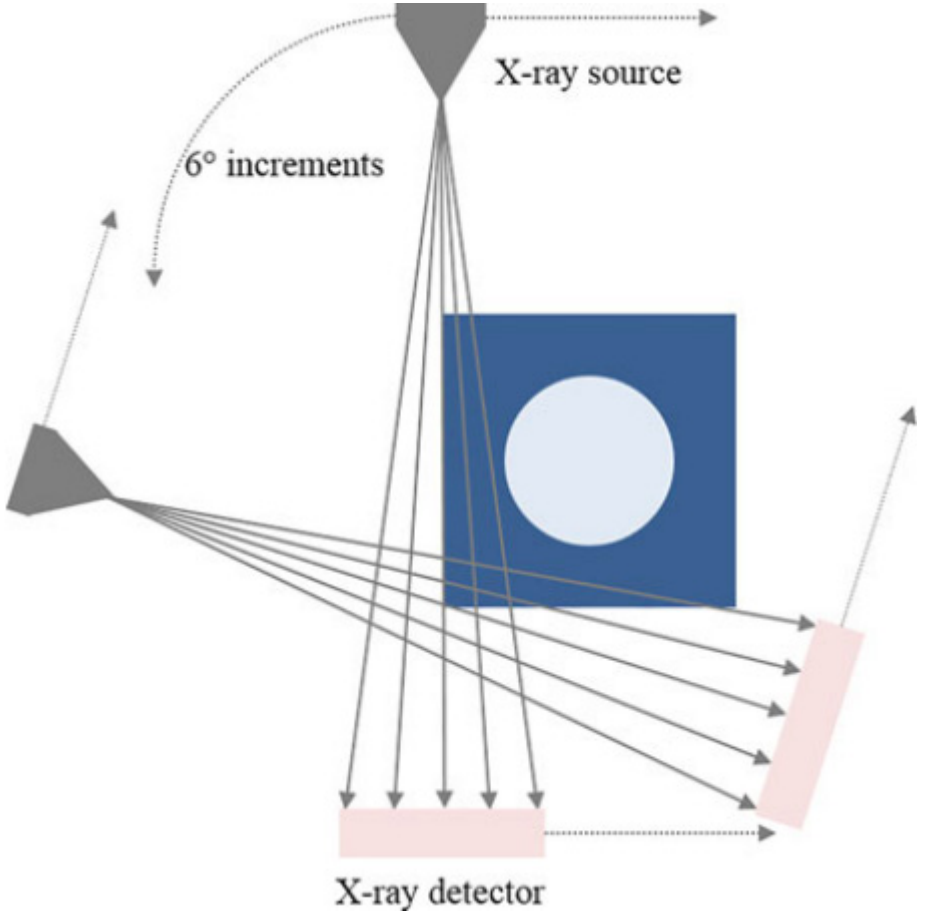

History of clinical CT scanners

The third generation of CT scanner, the first fan-beam type scanner.

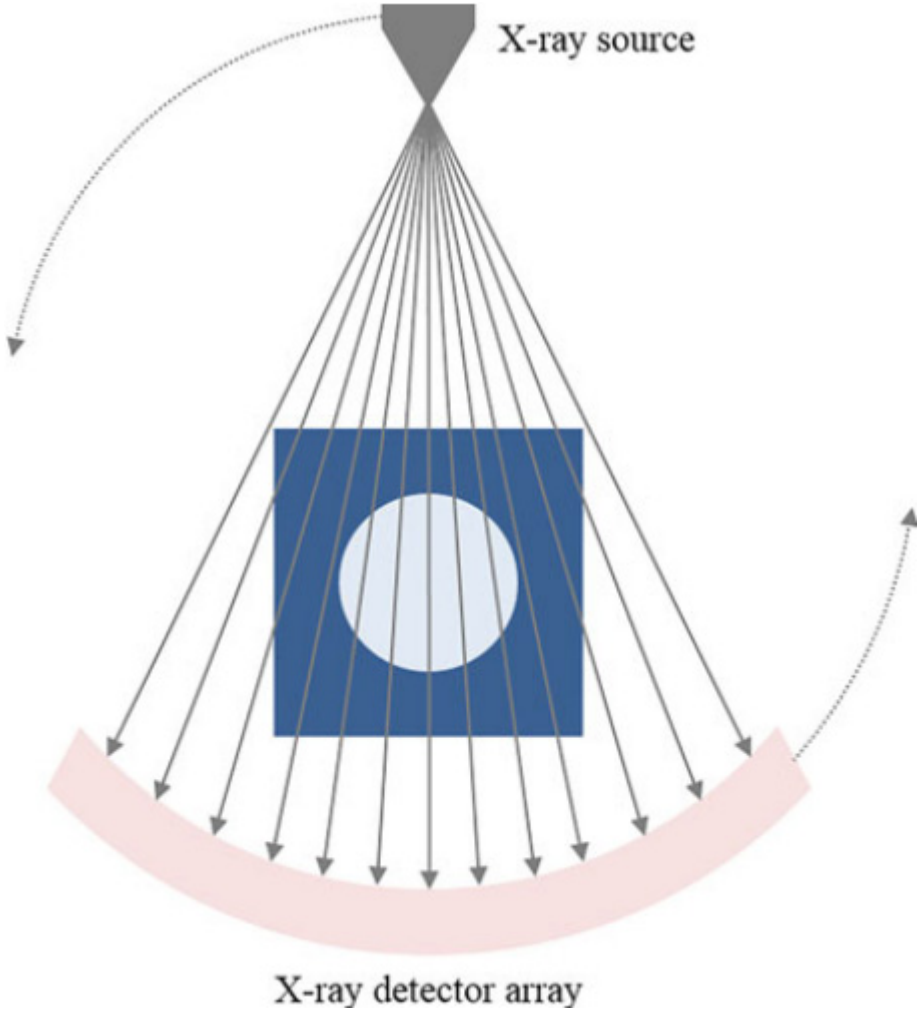

History of clinical CT scanners

A fourth generation CT scanner, showing the full ring of detector elements.

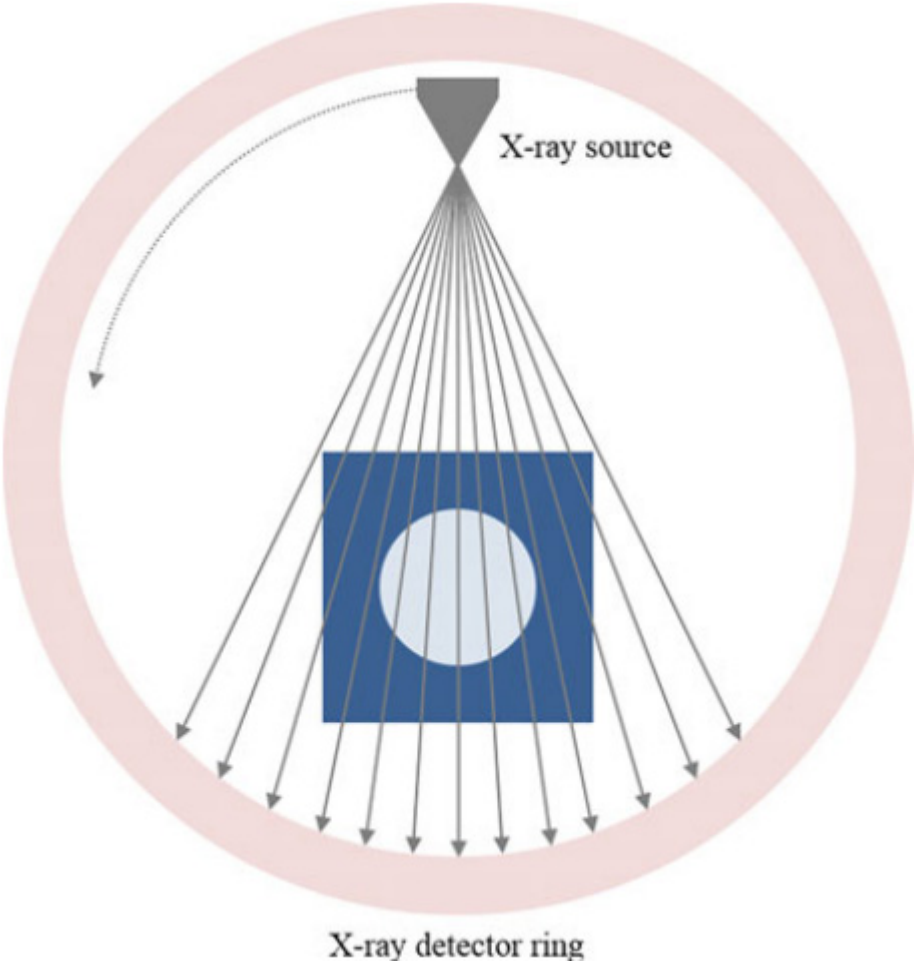

History of clinical CT scanners

The fifth generation CT scanner. The source and detector rings both sweep through angles of 210° and are arranged to be non-coplanar, so as to allow for the overlap

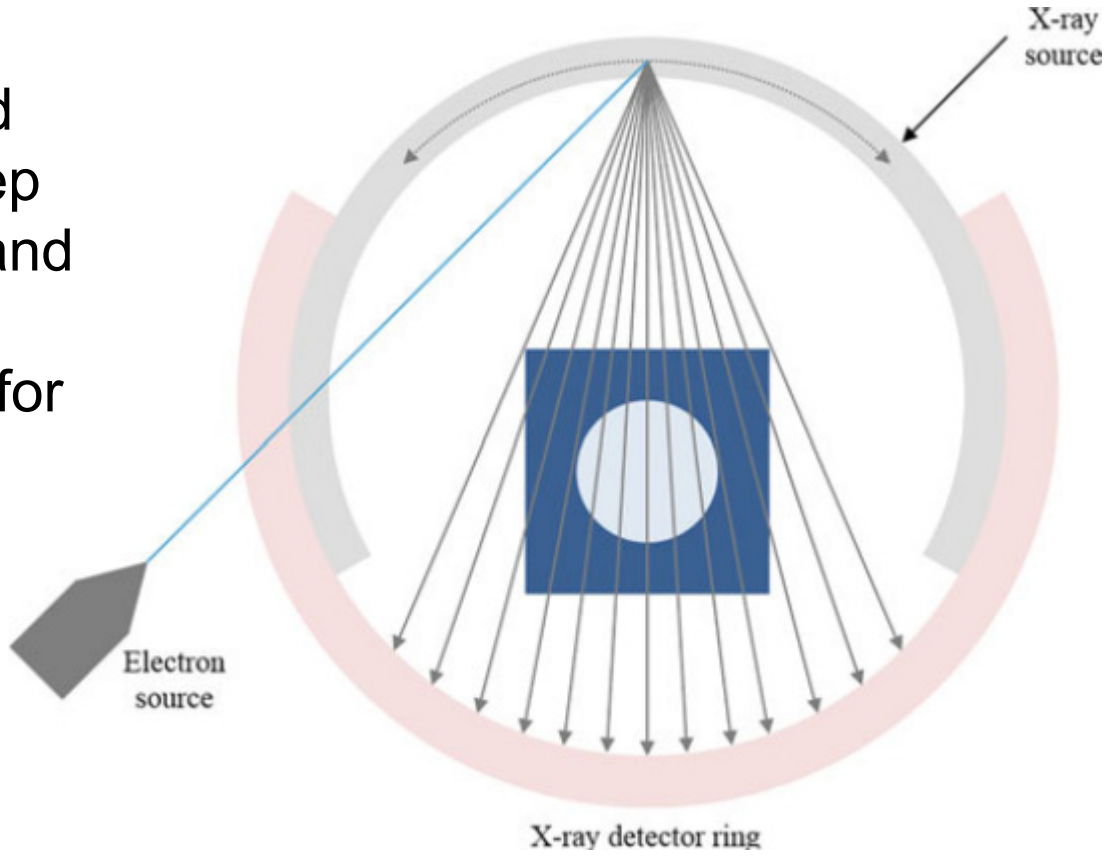

Mapping and reconstruction

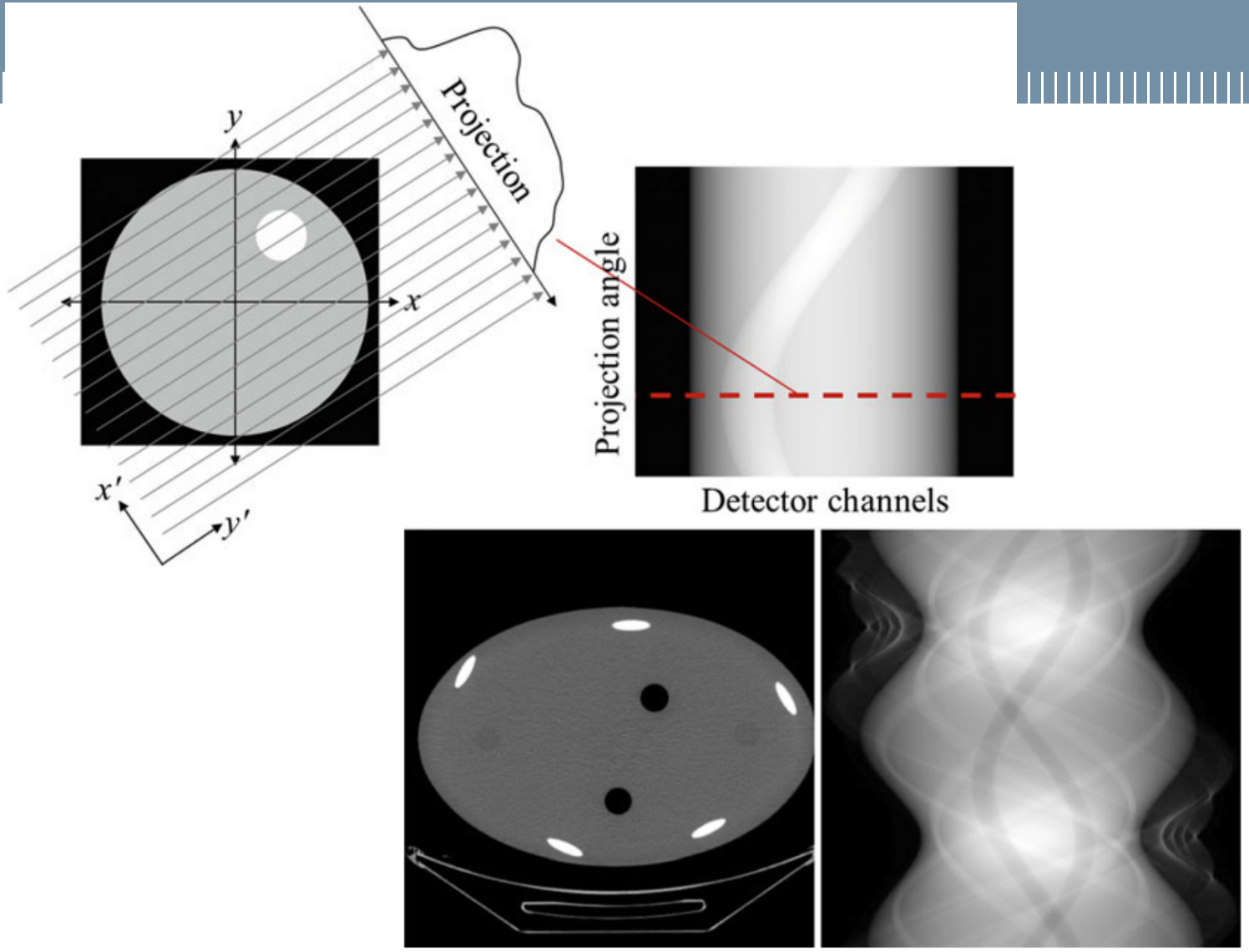

Image reconstruction

There are several techniques for performing image reconstruction, which can be classified into:

- Analytical,
- Algebraic,
- Statistical.

Analytical techniques model the object as a mathematical function, thus, reconstruct the object by solving a continuous integral equation.

- Analytical techniques are divided into:
  - exact algorithms
  - non-exact algorithms
- depending on whether or not the solution of the integral equation is exact.
- Algebraic Reconstruction Techniques (ARTs) make use of iterative reconstruction approaches in which several iterations are performed until certain criteria are met.
- Statistical reconstruction algorithms are also iterative methods, but in this case the unknowns are assigned by means of likelihood principles.

Fourier Slice Theorem

The object, which in this case for simplicity is represented as a circle in the 2D view, is described by the function f(x,y).
Coordinate system used for the tomographic reconstruction in parallel-beam geometry:

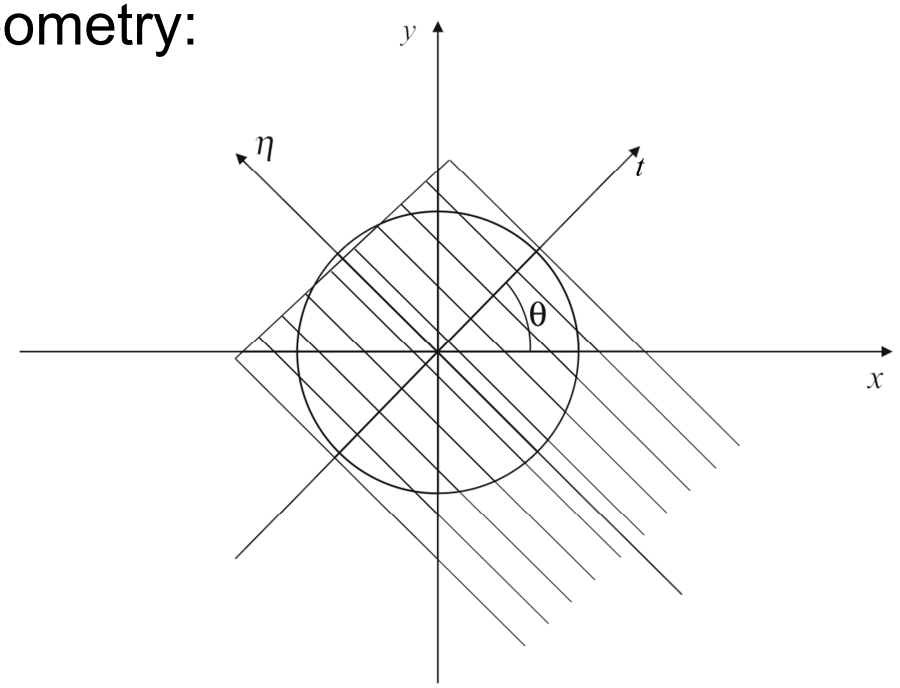

Fourier Slice Theorem

The object, which in this case for simplicity is represented as a circle in the 2D view, is described by the function f(x,y).
Coordinate system used for the tomographic reconstruction in parallel-beam geometry:

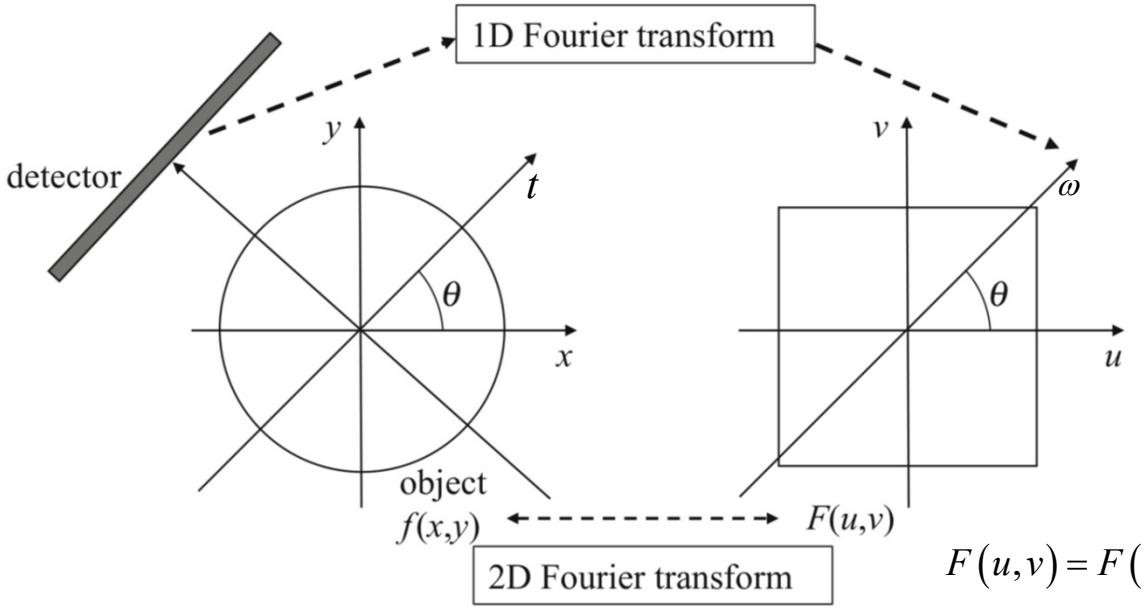

$$F(u,v) = F(\omega\cos\theta, \omega\sin\theta)$$

Fourier Slice Theorem

If $P_\theta(\omega) = \mathcal{F}\{p_\theta(t)\}$ is the 1D Fourier transform in the θ direction (ω represents frequencies along that direction), then it also corresponds to the values of the 2D Fourier transform along the straight line: $u\sin\theta - v\cos\theta = 0$

and, in particular, $\omega = u\cos\theta + v\sin\theta$

- Fourier slice theorem provides a straightforward procedure for tomographic reconstruction, but,in the practical implementation, after applying the 1D Fourier transform to each projection, the Fourier space is filled on a polar coordinate grid.
- The fast Fourier transform (FFT), however,requires data on a Cartesian grid.
- For performing the 2D inverse Radon transform by means of a FFT algorithm, a regridding process is required in which projection data are rearranged from a polar to a Cartesian grid through interpolation.
- Interpolation in the frequency domain is not as straightforward as in the spatial domain, and is difficult to implement.

Filtered Backprojection

The FBP algorithm, is the most widely used reconstruction method, directly derived from the Fourier Slice Theorem.

Each projection describes the distribution of the attenuation coefficient for the given X-ray path.

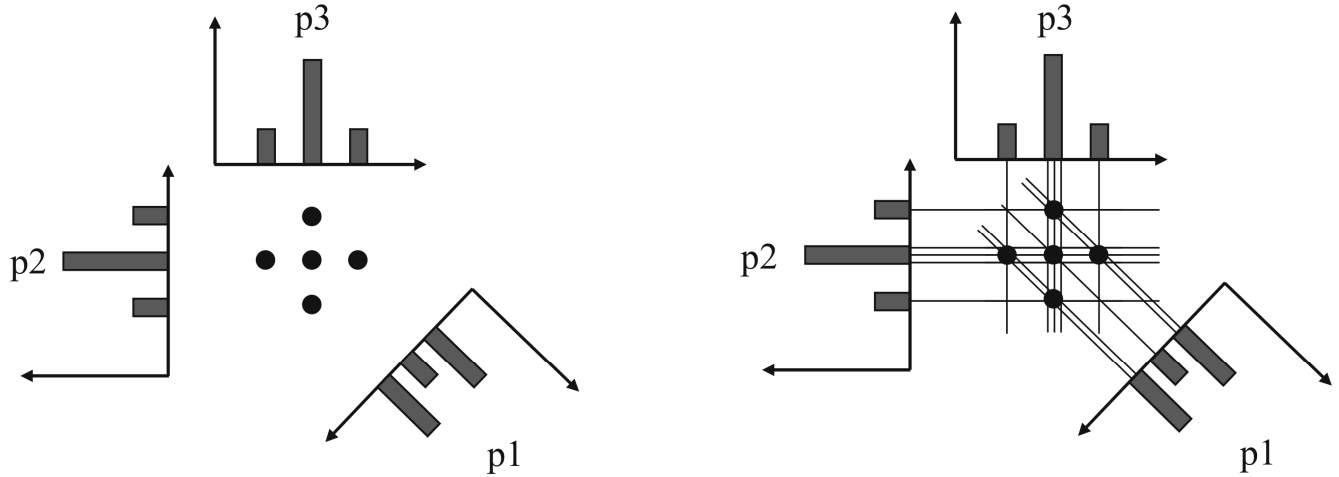

According to the simple backprojection principle, every profile is backprojected along the viewing direction (i.e. the θ angle) from which it was acquired.

Backprojection blurring

Due to the fact that each projection is a non-negative function, positive values are also assigned to voxels that do not contain the object. This leads to a blurred image that is not of sufficient quality.

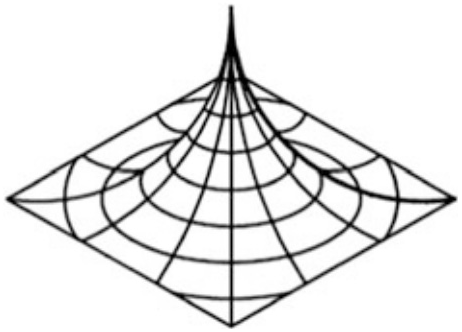

The figure represents the result of the simple backprojection of a point object.

The superimposed profiles produce a central spike with a broad skirt that falls off as 1/r.

Implementation of the Filtered Back Propagation

FBP involves convolving each object projection with

a filtering function (directly obtained from the polar coordinates), before calculating the inverse Fourier transform to recover the object.

The 2D inverse Fourier Transform is:

$$f(x,y)=\int_{-\infty}^{\infty}\int_{-\infty}^{\infty}F(u,v)e^{j2\pi(ux+vy)}dudv$$

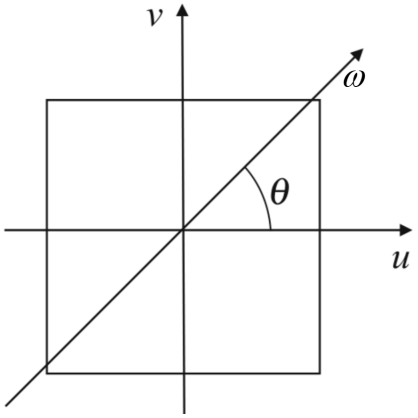

Since

$$u=\omega\cos\theta,\quad v=\omega\sin\theta,\quad \omega=\sqrt{u^2+v^2},\quad \theta=\tan^{-1}(v/u)$$

The differentials can be changed in: $dudv=\omega d\omega d\theta$

$$f(x,y)=\int_{0}^{2\pi}\int_{0}^{\infty}F(\omega,\theta)e^{j2\pi\omega(x\cos\theta+y\sin\theta)}\omega d\omega d\theta$$

Implementation of the Filtered Back Propagation

$$f(x,y) = \int_0^{2\pi} \int_0^{\infty} F(\omega,\theta) e^{j2\pi\omega(x\cos\theta + y\sin\theta)} \omega d\omega d\theta$$

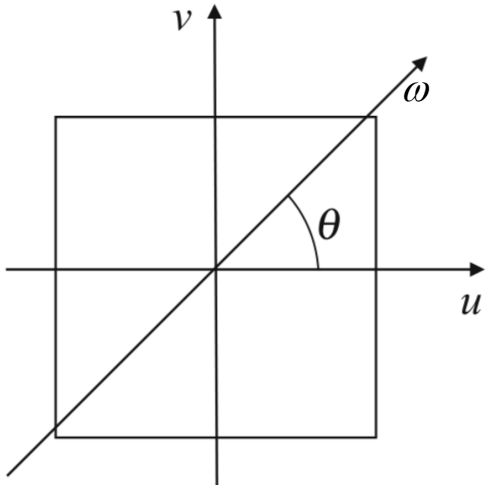

The formula is equivalent to:

$$f(x,y) = \int_0^{\pi} \left[\int_{-\infty}^{\infty} F(\omega,\theta) e^{j2\pi\omega(x\cos\theta + y\sin\theta)} |\omega| d\omega \right] d\theta$$

So, we can limit the values of $F(\omega,\theta)$ to the acquired values $P_\theta(\omega) = \mathcal{F}\{p_\theta(t)\}$

$$f(x,y) = \int_0^{\pi} \left[\int_{-\infty}^{\infty} P_\theta(\omega) |\omega| e^{j2\pi\omega(x\cos\theta + y\sin\theta)} d\omega \right] d\theta$$

Implementation of the Filtered Back Propagation

$$f(x,y)=\int_0^{\pi}\left[\int_{-\infty}^{\infty}P_\theta(\omega)|\omega|e^{j2\pi\omega(x\cos\theta+y\sin\theta)}d\omega\right]d\theta$$

The formula is equivalent to:

$$f(x,y)=\int_0^{\pi}\left[\int_{-\infty}^{\infty}\mathcal{F}\{p_\theta(t)\}|\omega|e^{j2\pi\omega(x\cos\theta+y\sin\theta)}d\omega\right]d\theta$$

That, in a discrete formulation (finite number I of views θ_i) becomes:

$$f(x,y)=\frac{\pi}{I}\sum_{i=1}^{I}\mathcal{F}^{-1}\left\{\mathcal{F}\{p_{\theta_i}(t)\}|\omega|\right\}$$

Continuous and discrete reconstruction with FBP

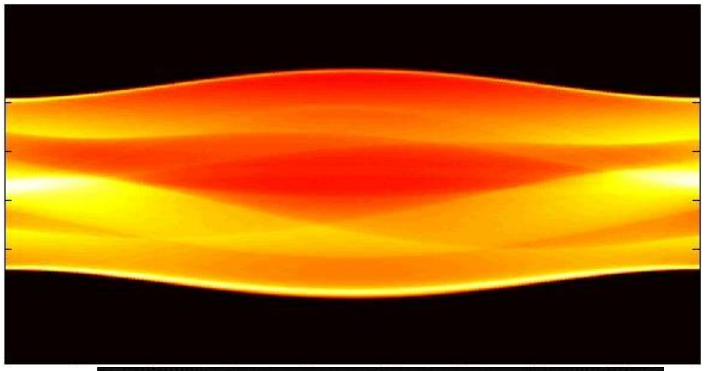

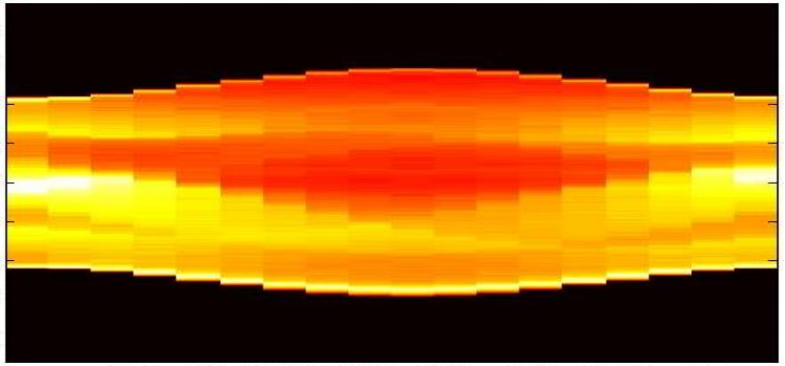

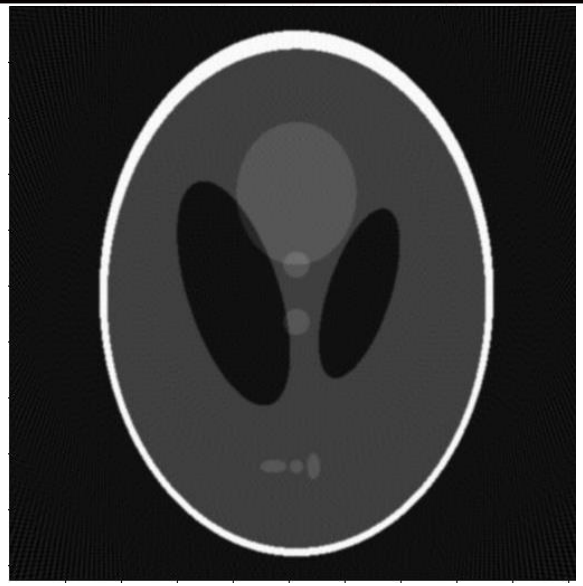

Algebraic reconstruction technique

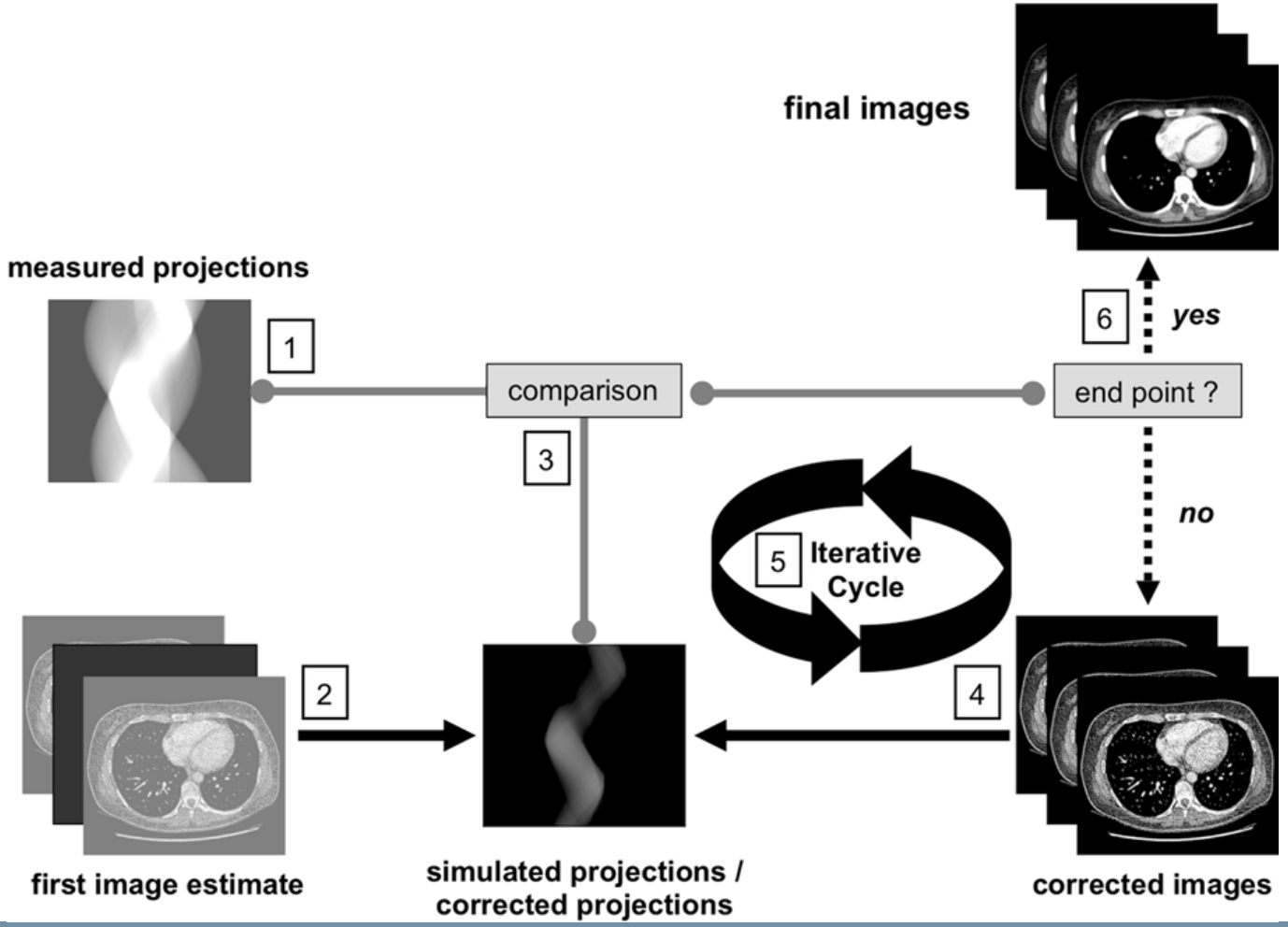

Algebraic Reconstruction Technique

An advantage of ART over other reconstruction methods (such as filtered backprojection) is that it is relatively easy to incorporate prior knowledge into the reconstruction process.

$$Ax = b$$

ART can be considered as an iterative solver of a system of linear equations where:

- A is a sparse $m \times n$ matrix whose values represent the relative contribution of each output pixel to different points in the sinogram (m being the number of individual values in the sinogram, and n being the number of output pixels);
- x represents the pixels in the generated (output) image, arranged as a vector, and:
- b is a vector representing the sinogram. Each projection (row) in the sinogram is made up of a number of discrete values, arranged along the transverse axis.

b is made up of all of these values, from each of the individual projections.

Algebraic Reconstruction Technique

Given a real or complex matrix A and a real or complex vector b, respectively, the method computes an approximation of the solution of the linear systems of equations as in the following formula

$$x^{k+1} = x^k + \lambda_k \frac{b_i - \langle a_i, x^k \rangle}{\|a_i\|^2} a_i^{\mathsf{T}}$$

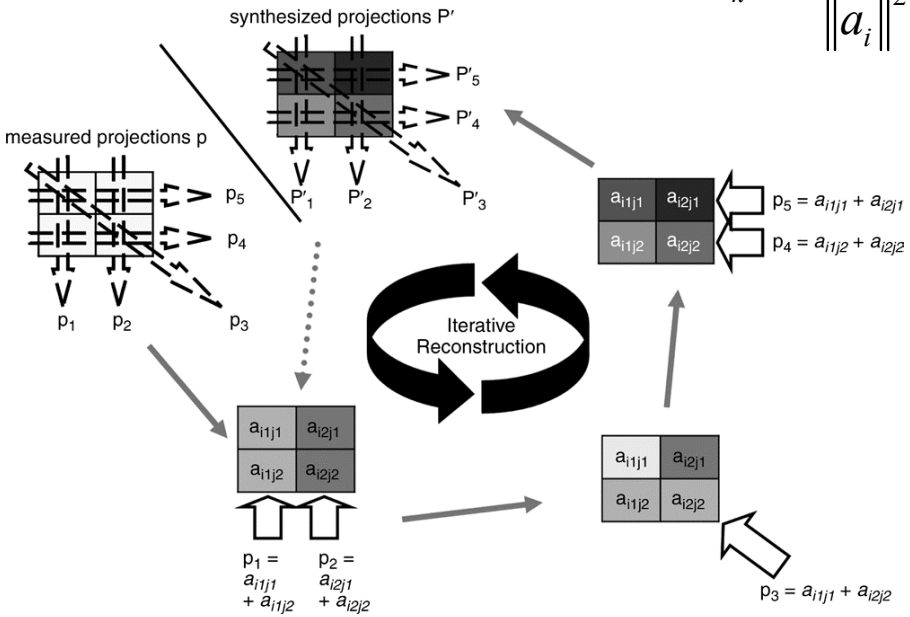

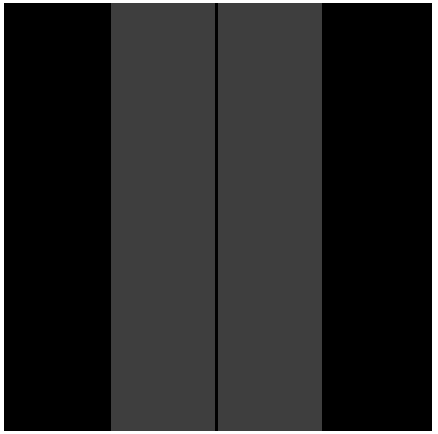

Dominant reconstruction approaches

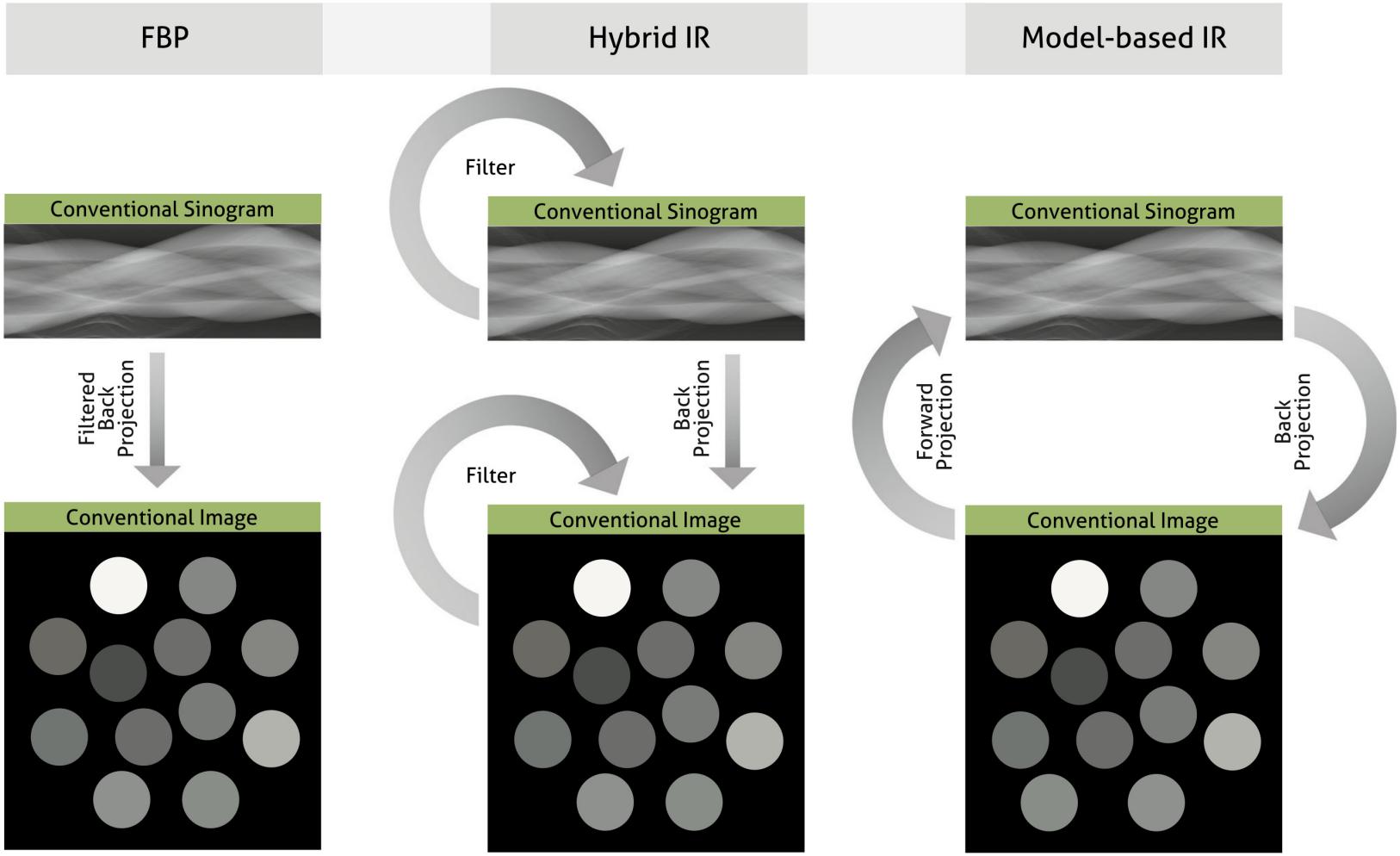

Ex vivo human heart scanned at 4 mGy and 1 mGy

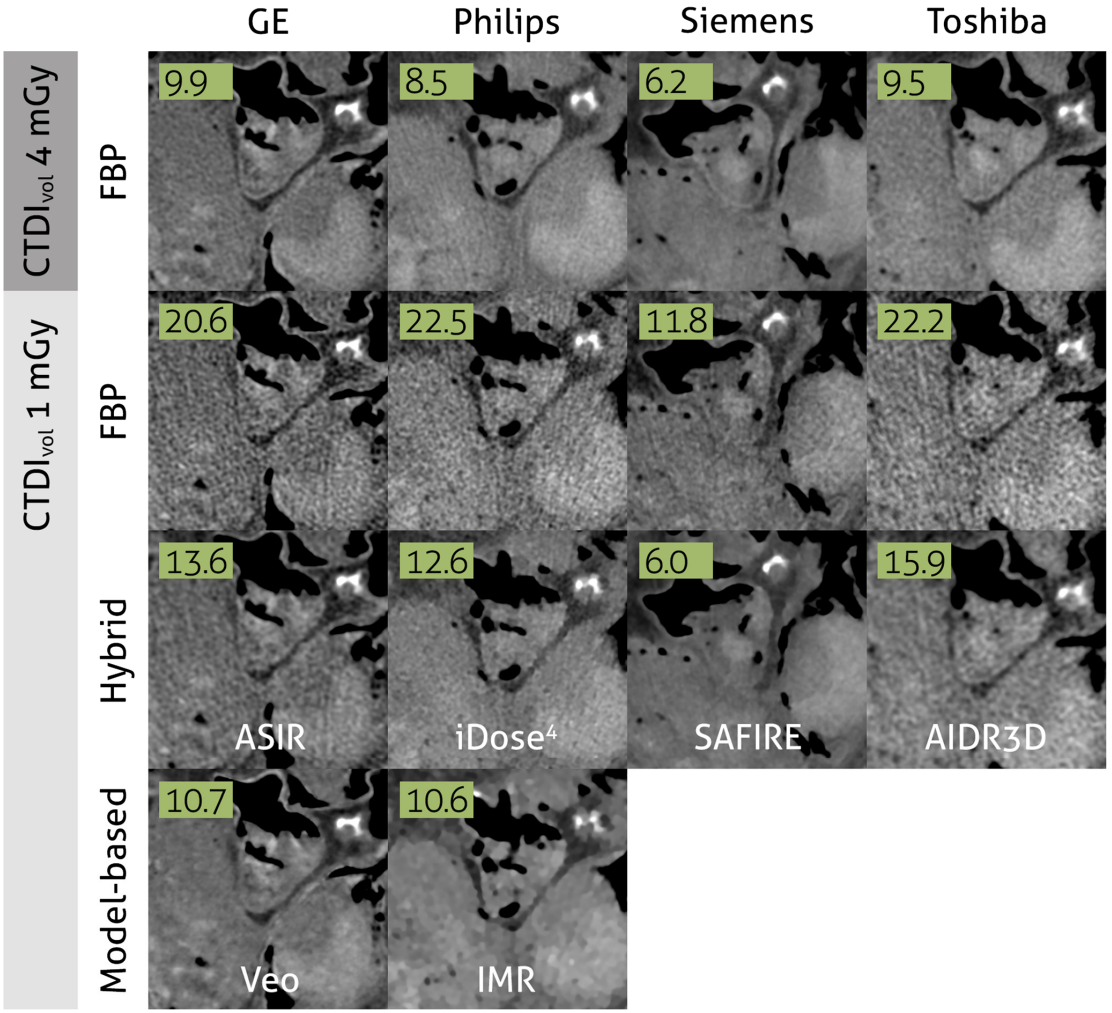

Multi band tomography

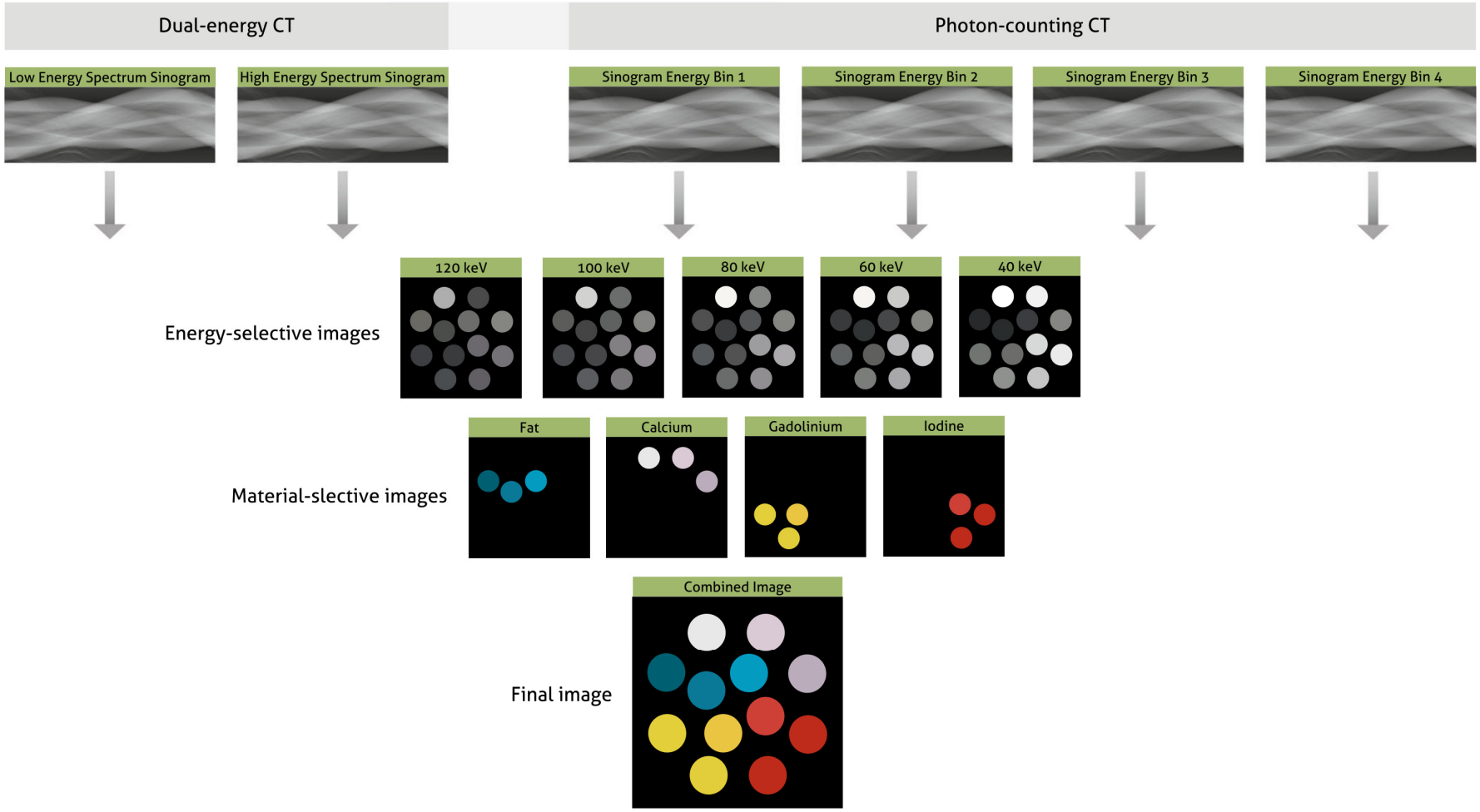

The Hyperspectral image tensor

Using the MultiX ME100 a detailed description of the analyzed foods is obtained in a wide (0-160keV) photon energy range.

The following analysis is performed on the image tensor where every pixel is described as a set of 128 '*colors*' i.e. the energy bins that represent the spectrum of the acquired point.

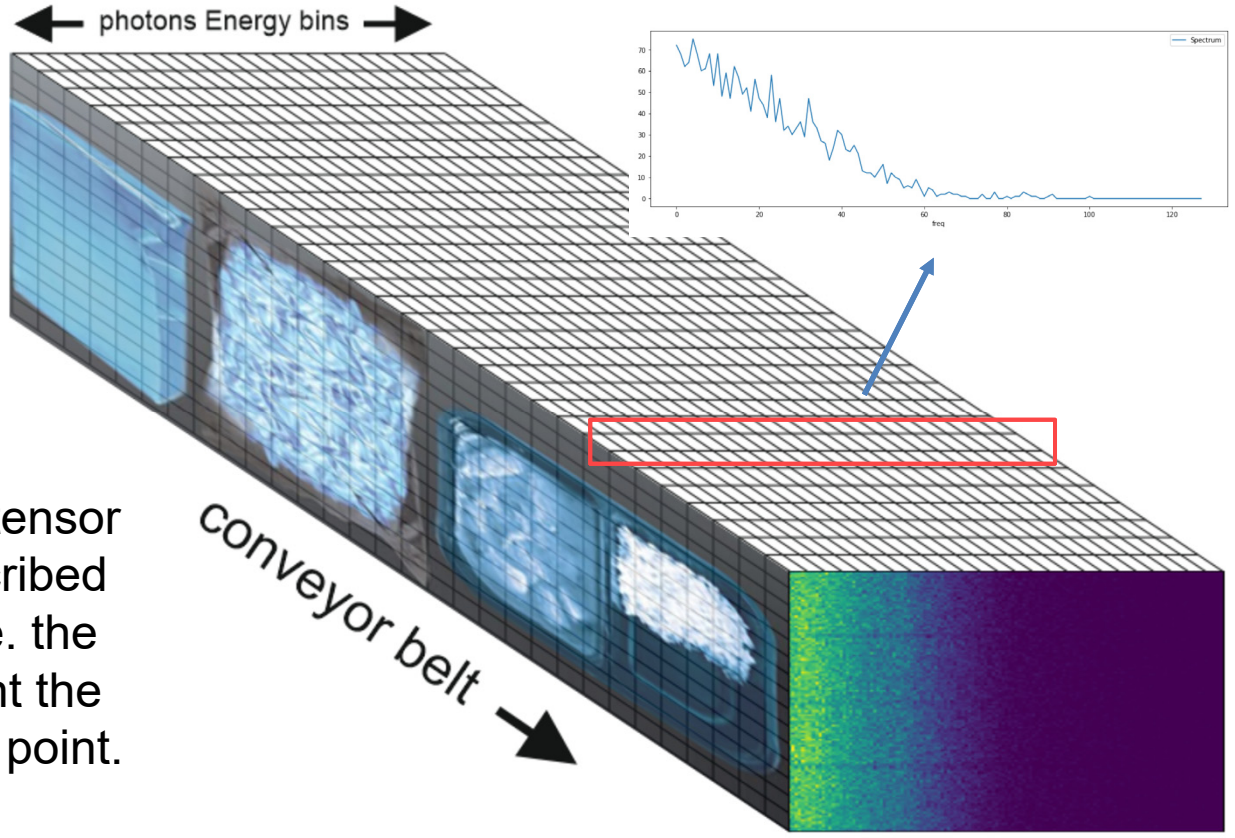

Multi energy detectors vs. conventional detectors

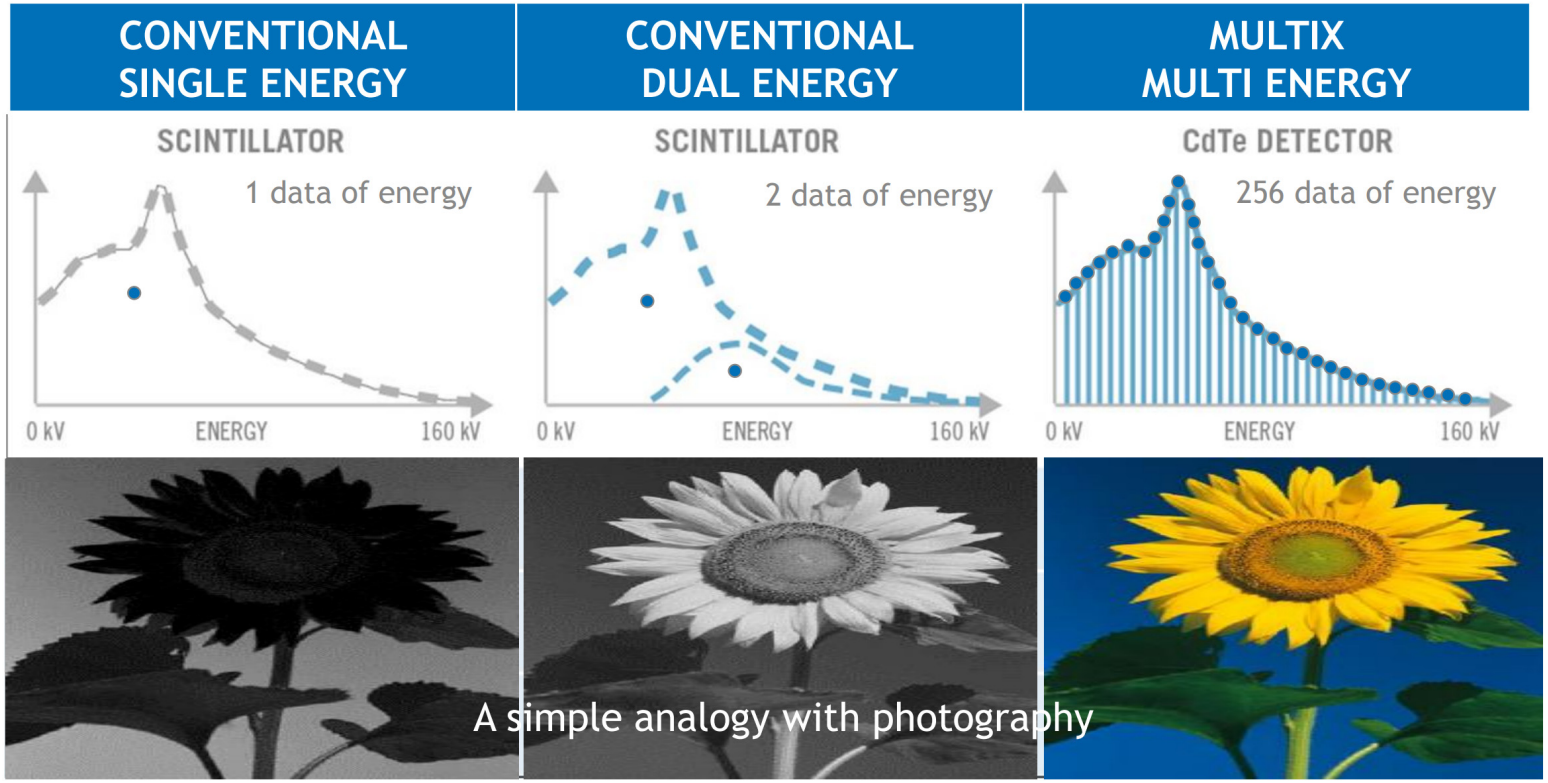

Multi energy demonstrates a much better capability to segregate materials with close atomic composition

The classification phase

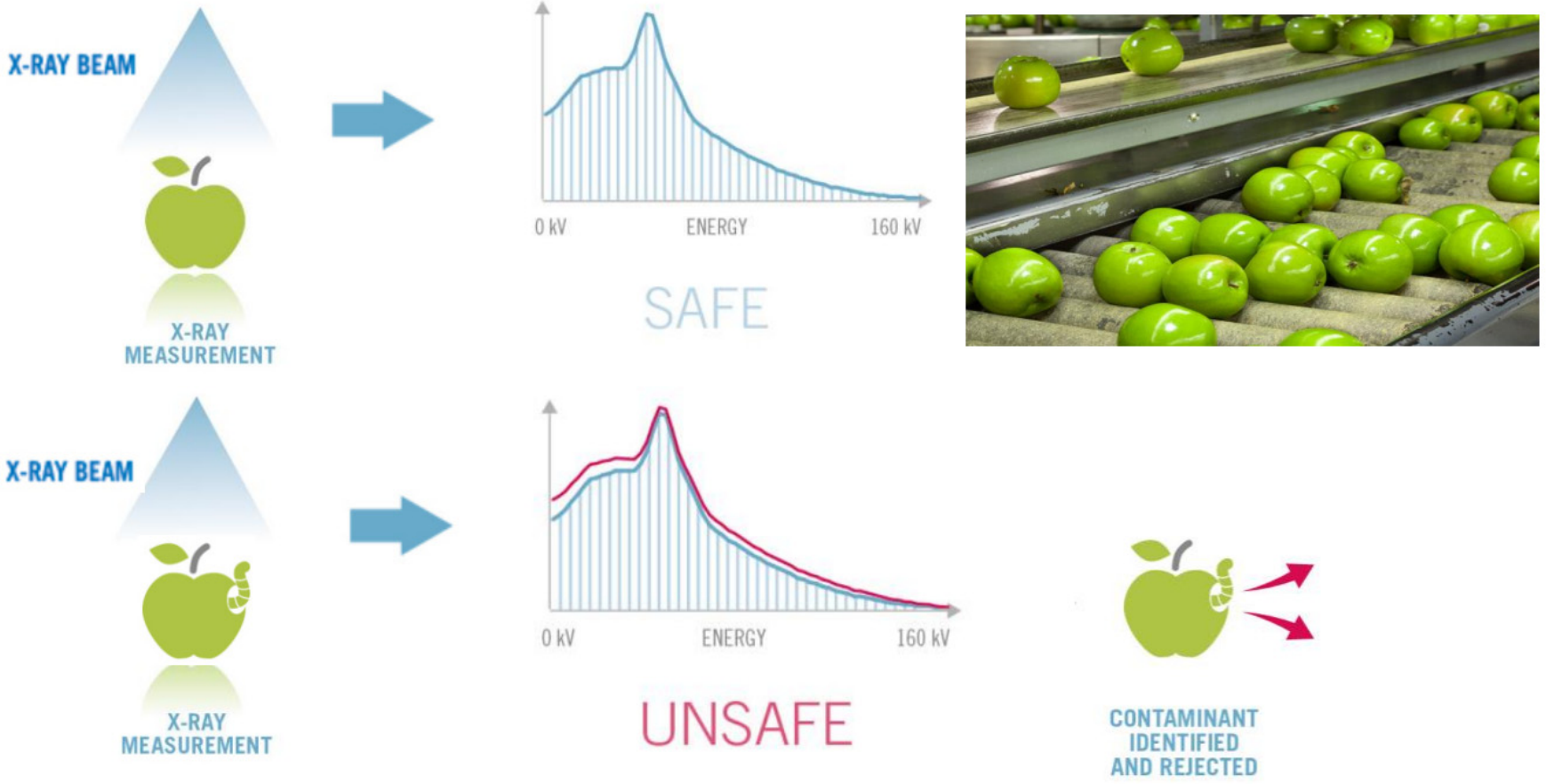

Phase-Contrast Tomography

Working principle:

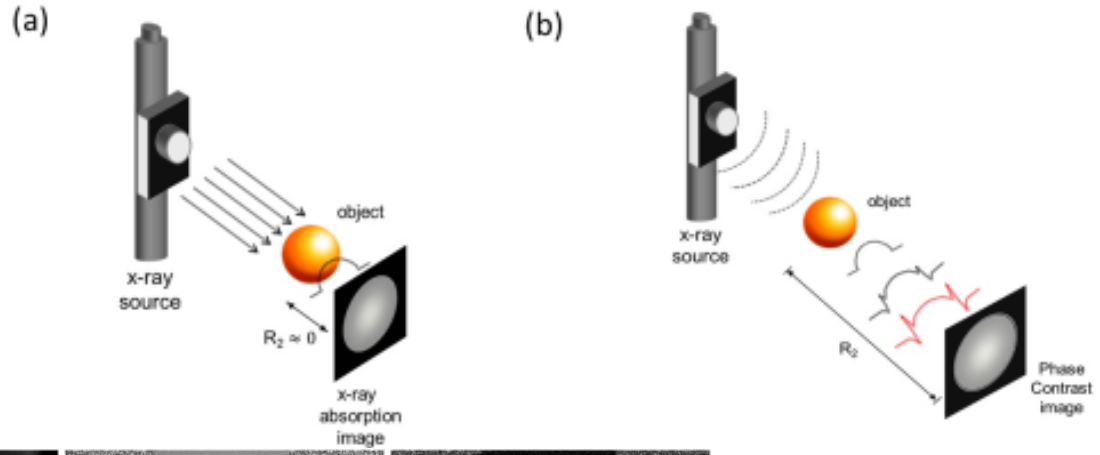

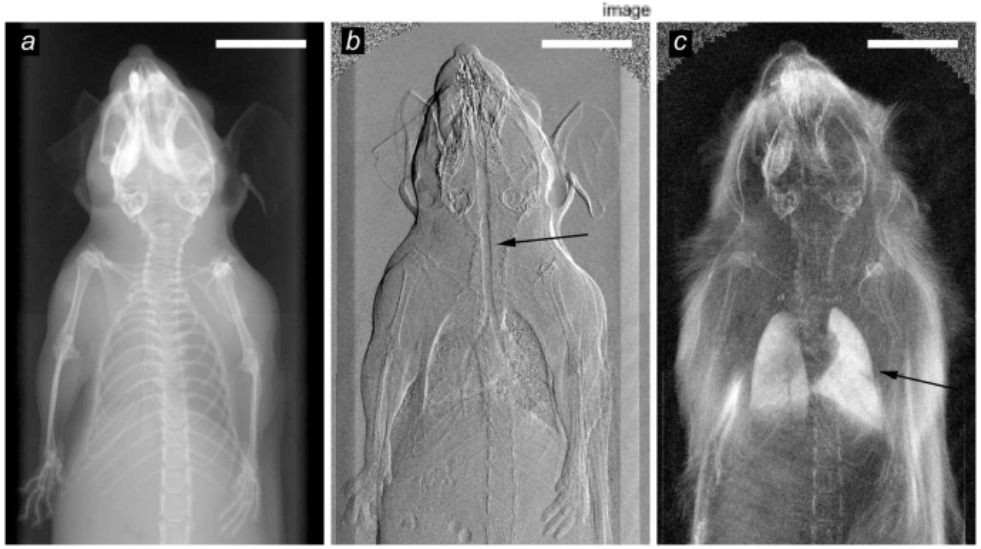

Phase-Contrast Tomography

Phase-contrast X-ray imaging is a general term for that use information concerning changes in the phase of an X-ray beam that passes through an object in order to create its images.

Standard X-ray imaging techniques rely on a decrease of the X-ray beam's intensity (attenuation) when traversing the sample, it can can be measured directly with the assistance of an X-ray detector.

In phase contrast X-ray imaging, the beam's phase shift caused by the sample is not measured directly, but is transformed into variations in intensity, which then can be recorded by the detector.

Phase contrast imaging can be combined with tomographic techniques to obtain the 3D distribution of the real part of the refractive index of the sample.

Wave propagation

For X-rays the complex refractive index of a medium is typically written as:

$$n = 1 - \underbrace{\delta}_{elastic} + \underbrace{i\beta}_{inelastic} \qquad \text{with } \delta << 1$$

A planar wave in vacuum can be written as:

$$\Psi_v(\vec{r}, t) = \Psi_0 \, e^{i(\vec{k}\vec{r} - \omega t)} = \Psi_0 \, e^{i(kz - \omega t)}$$

where:

$$\vec{k} = (0, 0, k = \tfrac{2\pi}{\lambda})$$

While, in a medium:

$$\Psi_m(z, t) = \Psi_0 \, e^{i(nkz - \omega t)} = \Psi_0 \, e^{-i\omega t} \, e^{(1-\delta)ikz} \, e^{-\beta kz} = \Psi_v(z, t) \cdot \underbrace{e^{-i\delta kz}}_{\text{[phase-shift]}} \cdot \underbrace{e^{-\beta kz}}_{\text{[attenuation]}}$$

Phase propagation

(a) When a wave-front travels through a medium with complex refractive index *n*, it experiences a decrease in wave-amplitude by ΔA as indicated by blue arrows, which is associated with the imaginary part of the refractive index.
The perturbed wave receives a shift in the wave-phase by $\Delta\Phi$ as indicated by red arrows, which is associated with the decrement of refractive index.

(b) When a wave-front travels through a phase prism (β = 0), a local variation in wave-shift implies a refraction of the wave by an angle αx, with respect to the incident wave-front. Note that peaks of the excited waves are aligned on a line (dashed line), which is titled by the angle αx with respect to the horizontal.

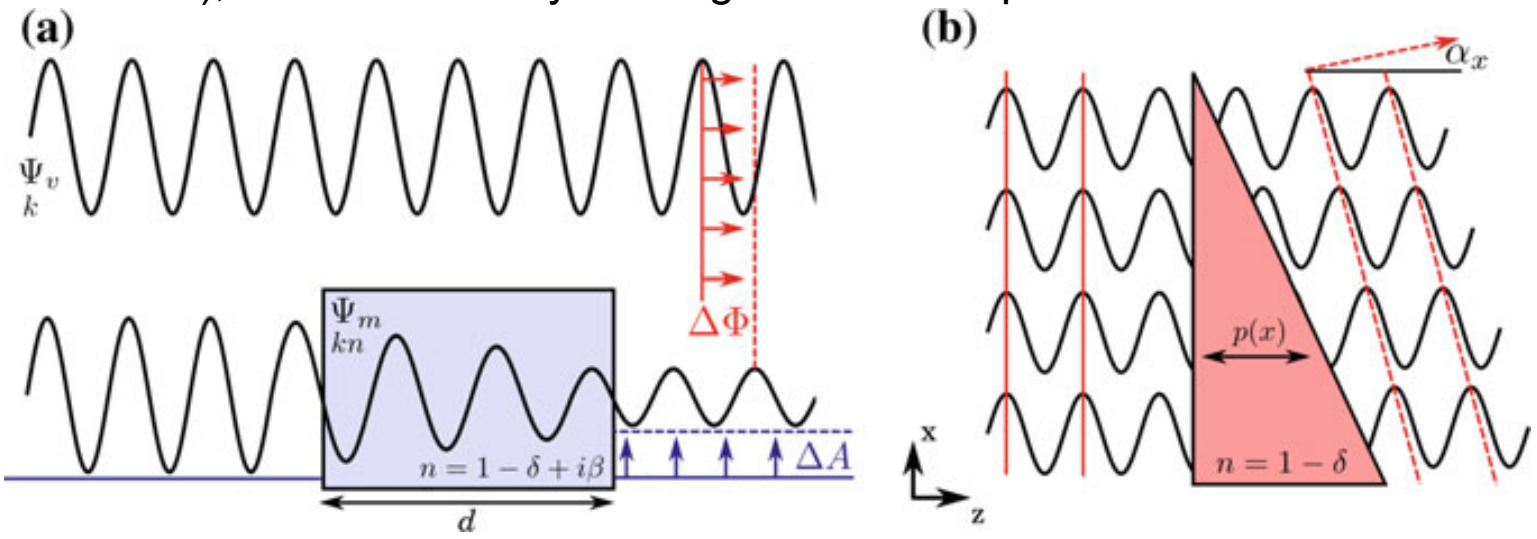

Attenuation of X-rays

The ratio of beam intensities before and after the medium is:

$$T(d) = \frac{I_m(d)}{I_v(0)} = \frac{|\Psi_m(d,t)|^2}{|\Psi_v(0,t)|^2} = \mathrm{e}^{-2k\beta d}$$

Comparing with Lambert-Beer:

$$T(d) = \frac{I_m(d)}{I_v(0)} = \mathrm{e}^{-\mu d}$$

Results in: $\mu = 2k\beta$

The variations induced by the medium are:

$$T(x,y) = \mathrm{e}^{-2k\int \beta(x,y,z)\,dz},$$

$$\Delta\Phi(x,y) = k\int \delta(x,y,z)\,dz,$$

$$\alpha_x(x,y) = \frac{1}{k}\frac{\partial\Phi(x,y)}{\partial x} = \frac{\partial}{\partial x}\int \delta(x,y,z)\,dz.$$

Why phase contrast?

δ is approximately 3 orders of magnitude larger than β, their typical values being $10^{-6} - 10^{-7}$ and $10^{-9} - 10^{-10}$, respectively. This huge difference is the reason why phase-sensitive techniques can be advantageous over attenuation-based imaging.

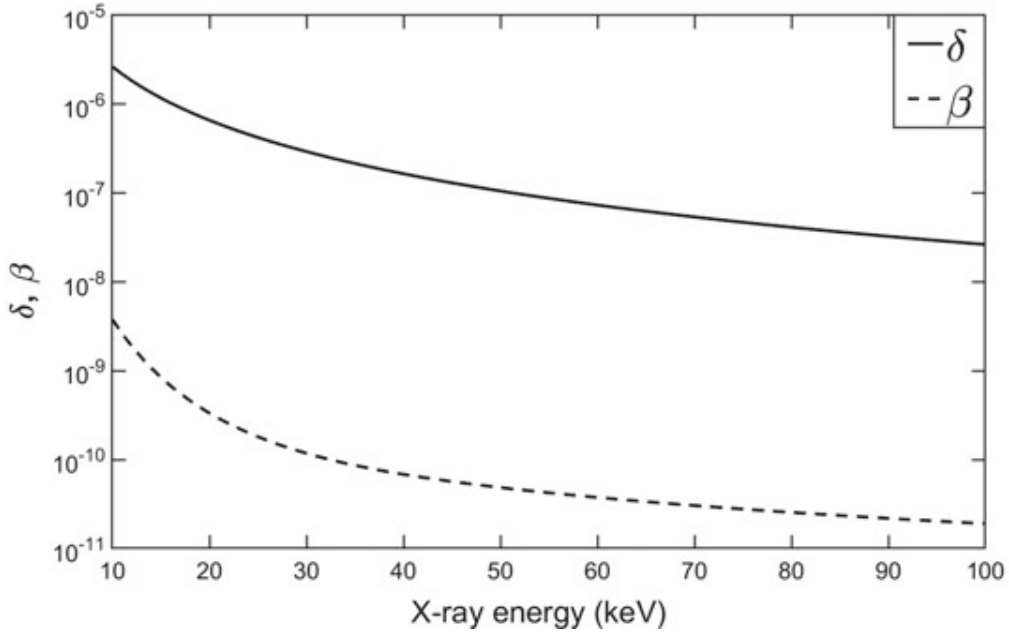

Phase contrast effect

Arrival points change:

$$\begin{cases} x_1 \simeq x + z_1 \alpha_x(x, y) \\ y_1 \simeq y + z_1 \alpha_y(x, y) \end{cases}$$

$$\alpha_x = \frac{1}{k}\frac{\partial}{\partial x}\Phi(x, y) \quad \text{and} \quad \alpha_y = \frac{1}{k}\frac{\partial}{\partial y}\Phi(x, y)$$

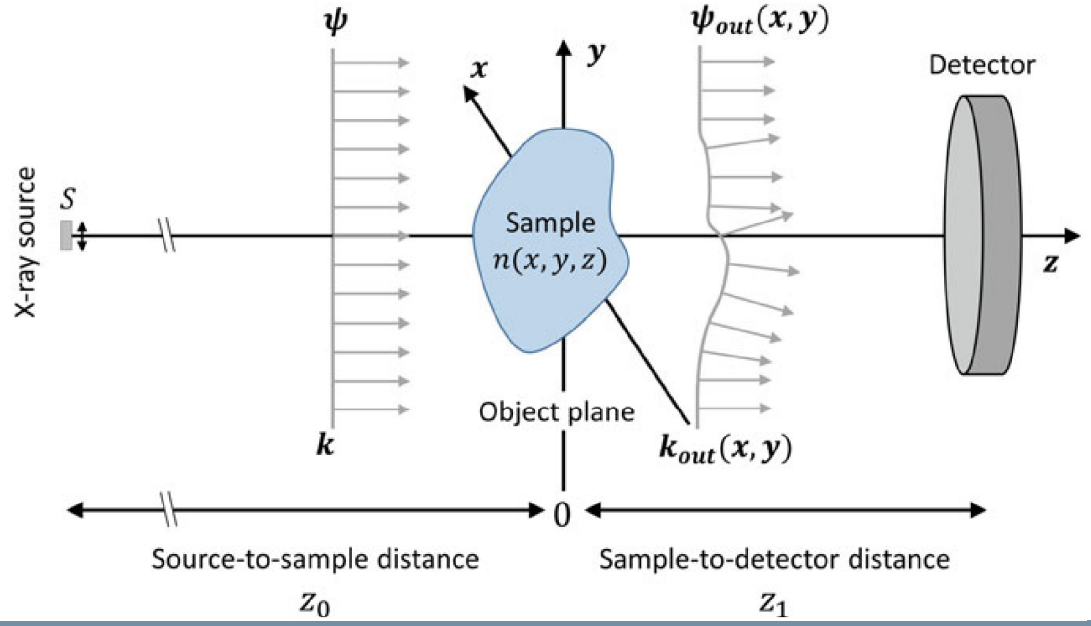

Intensity variation due to phase changes

$$
\begin{aligned}
I(x_1, y_1) &= I(x, y) \left| \frac{\partial(x_1, y_1)}{\partial(x, y)} \right|^{-1} \\
&= I(x, y) \begin{vmatrix} 1 + z_1 \frac{\partial \alpha_x}{\partial x} & z_1 \frac{\partial \alpha_x}{\partial y} \\ z_1 \frac{\partial \alpha_y}{\partial x} & 1 + z_1 \frac{\partial \alpha_y}{\partial y} \end{vmatrix}^{-1} \\
&\simeq I(x, y) \left(1 + \frac{z_1}{k} \nabla^2 \Phi(x, y) \right)^{-1}
\end{aligned}
$$

With a first-order Taylor expansion:

$$
\begin{aligned}
I(x_1, y_1) &\simeq I(x, y) \left(1 - \frac{z_1}{k} \nabla^2 \Phi(x, y) \right) \\
&= I_0 e^{-2k \int \beta(x,y,z)\, \mathrm{d}z} \left(1 - \frac{z_1}{k} \nabla^2 \Phi(x, y) \right)
\end{aligned}
$$

Phase Contrast results

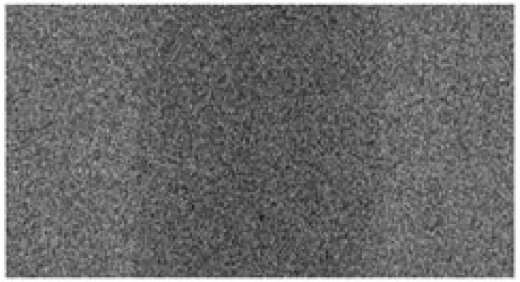

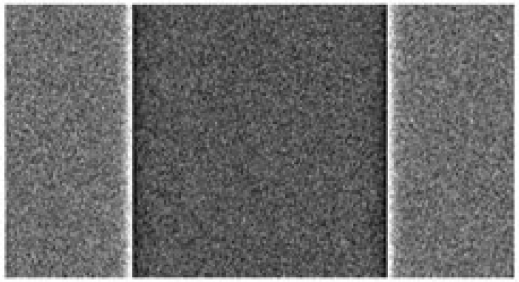

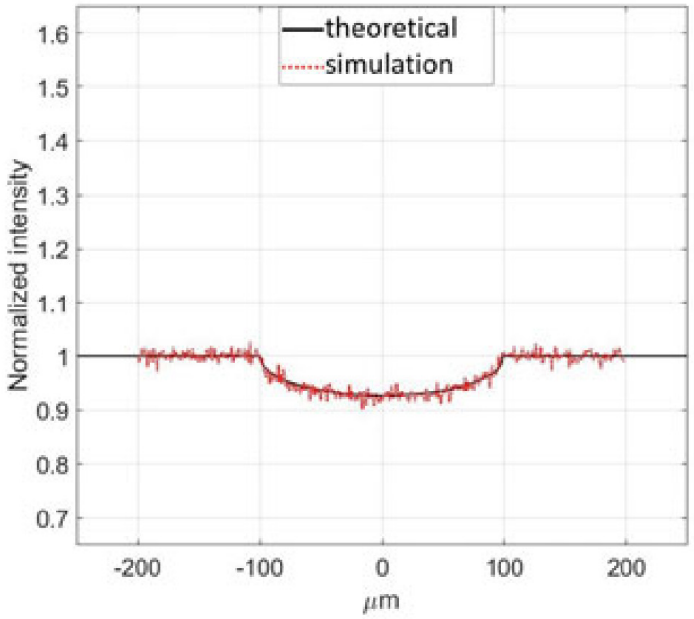

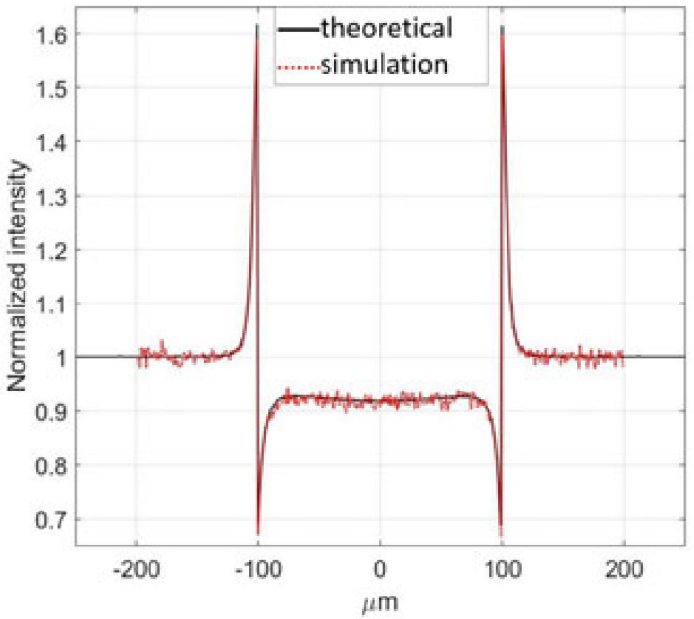

Intensity vs Phase contrast Tomography

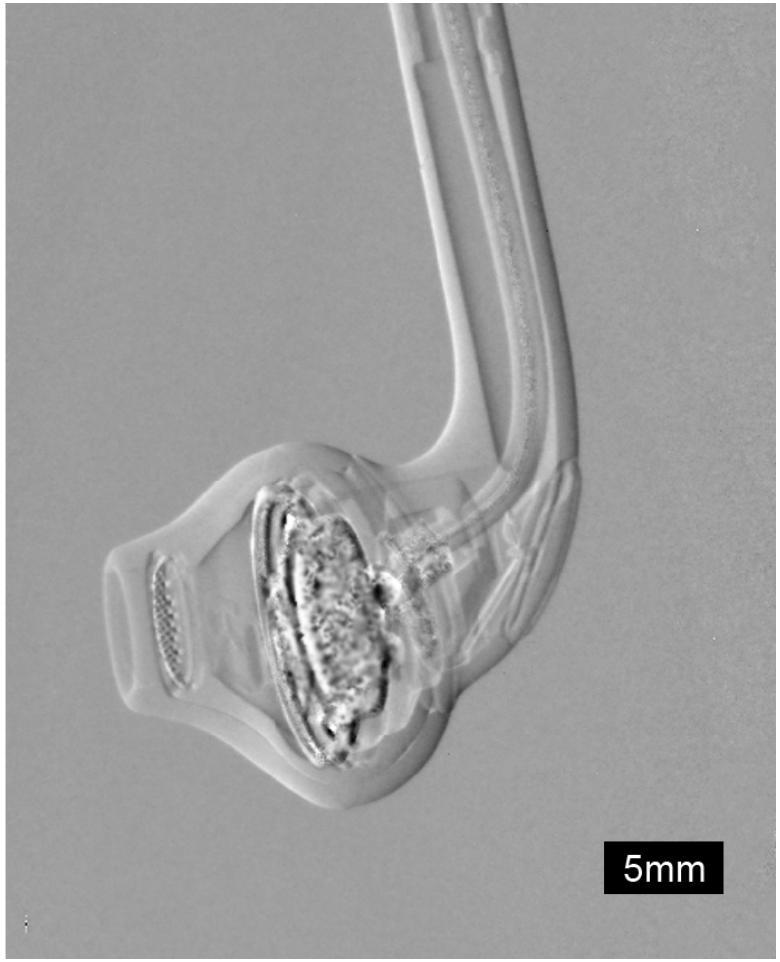

Intensity vs Phase contrast Tomography

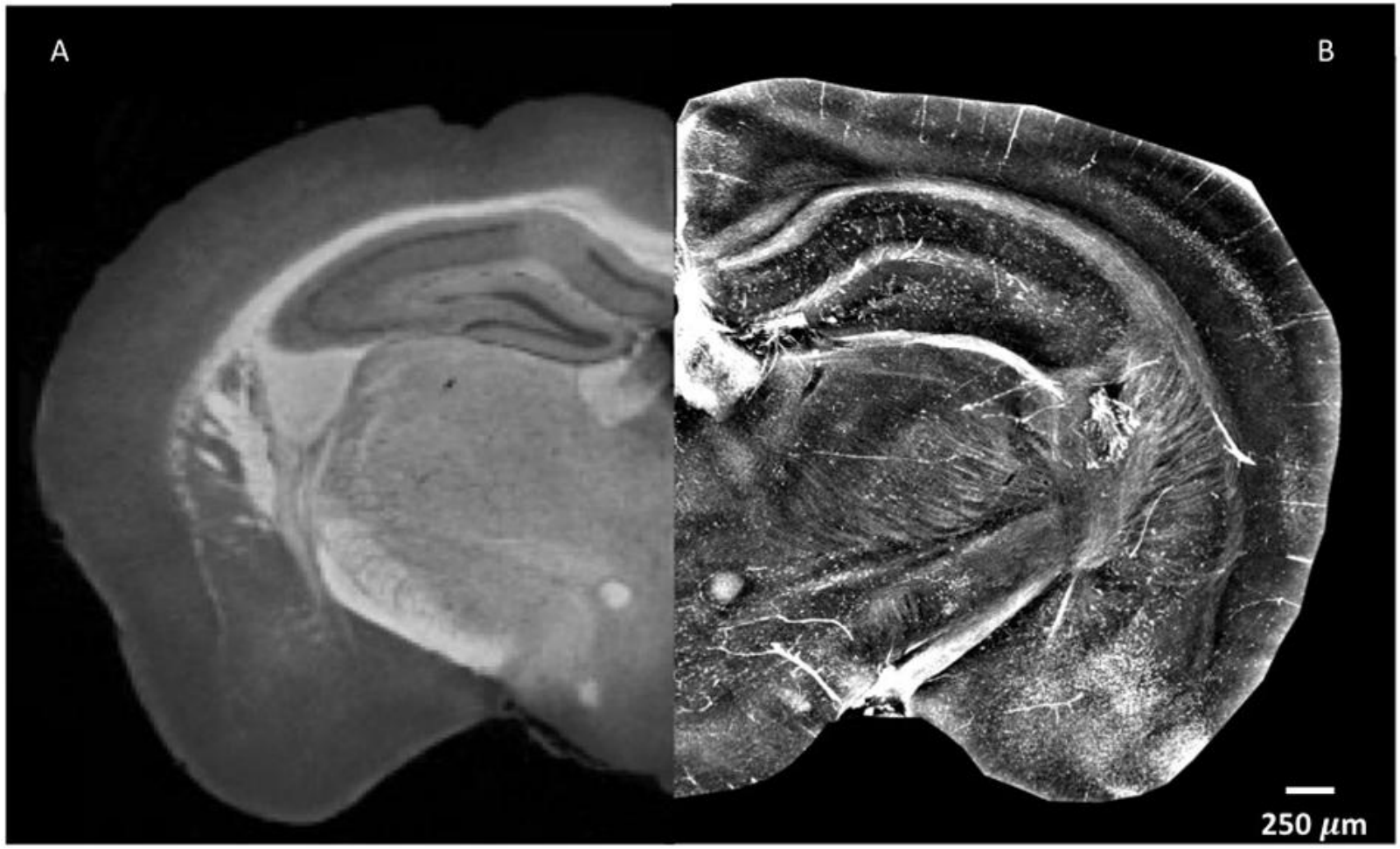

Intensity vs Phase contrast Tomography

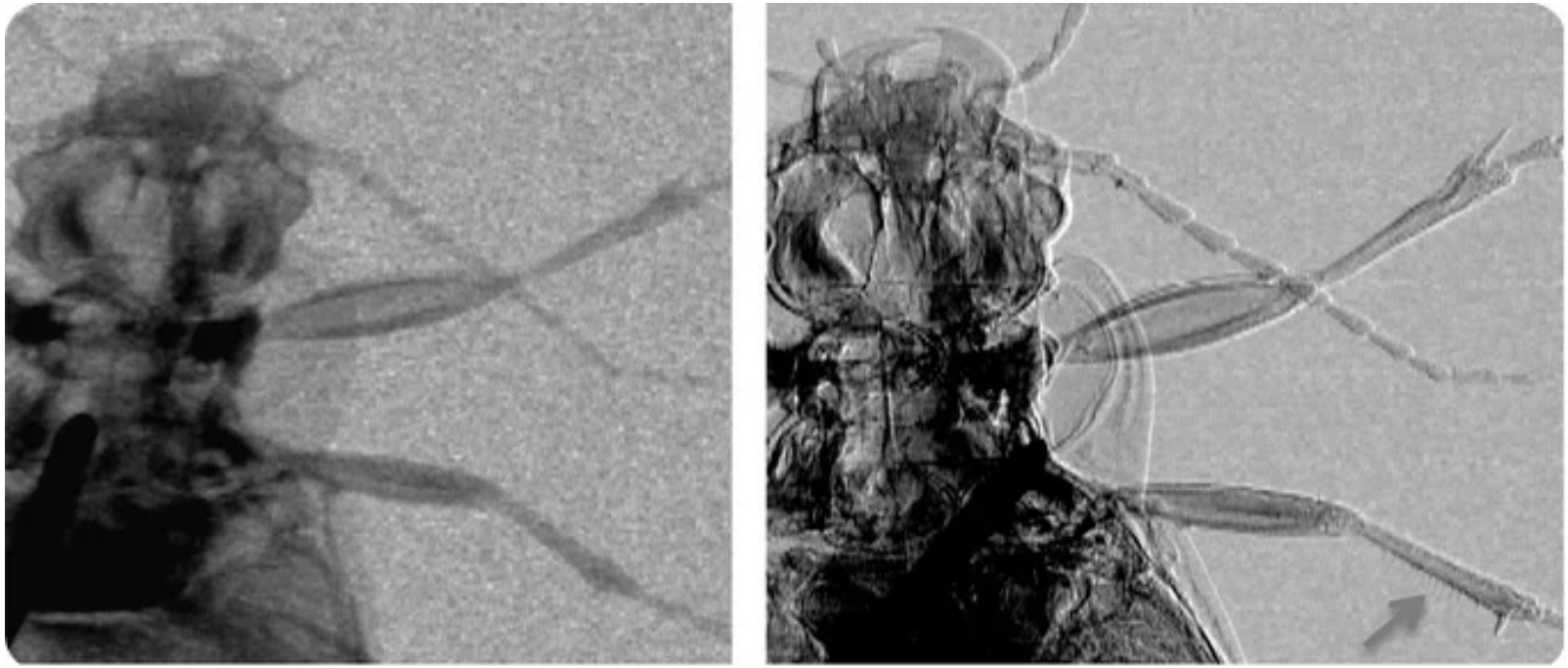

THE END